Science of the Total Environment 917 (2024) 170444

Contents lists available at ScienceDirect

Science of the Total Environment

journal homepage: www.elsevier.com/locate/scitotenv

Profiling dynamics of the Southeast Asia's largest lake, Tonle Sap Lake

Wenting Jiang [a], Zhijun Dai [a,b,*], Xuefei Mei [a], Chuqi Long [a], Nguyen An Binh [c], Cong Mai Van [d], Jinping Cheng [e]

[a] State Key Laboratory of Estuarine and Coastal Research, East China Normal University, Shanghai 200062, China
[b] Laboratory for Marine Geology, Qingdao National Laboratory for Marine Science and Technology, Qingdao 266061, China
[c] Ho Chi Minh City Institute of Resources Geography, Vietnam Academy of Science and Technology, Ho Chi Minh City, Viet Nam
[d] Faculty of Civil Engineering, Thuyloi University, Hanoi, Viet Nam
[e] Department of Science and Environmental Studies, The Education University of Hong Kong, New Territories, Hong Kong, China

HIGHLIGHTS

- Spatiotemporal change of the hydrological regime of the Tonle Sap Lake between 2000 and 2020.
- The water level of the Tonle Sap Lake showed no flooding during the flood season.
- A first assessment of the shoreline shrinkage rate of the Tonle Sap Lake over two decades.

GRAPHICAL ABSTRACT

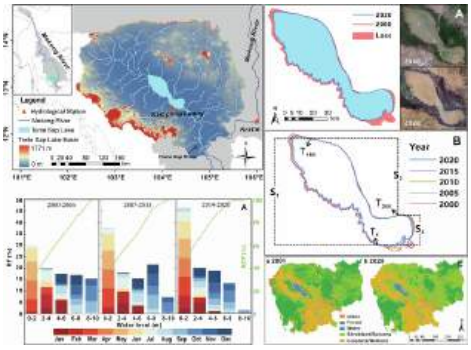

ARTICLE INFO

Editor: Ouyang Wei

Keywords:
Water level
Runoff
Shoreline
Lake dynamics
Human interferences
Tonle Sap Lake

ABSTRACT

Lakes, as vital components of the Earth's ecosystem with crucial roles in global biogeochemical cycles, are experiencing pervasive and irreparable worldwide losses due to natural factors and intensive anthropogenic interferences. In this study, we investigated the long-term dynamic patterns of the Tonle Sap Lake, the largest freshwater lake in the Mekong River Basin, using a series of hydrological data and remote sensing images between 2000 and 2020. Our findings revealed a significant decline in the annual average water level of the lake by approximately 2.1 m over 20 years, accompanied by an annual average reduction in surface area of about 1400 km^2. The Tonle Sap Lake exhibited episodic declines in water level and surface area, characterized by the absence of flooding during the flood season and increasing aridity during the dry season. Furthermore, the shoreline of the lake has significantly advanced towards the lake in the northwestern and southern regions during the dry season, primarily due to sedimentation-induced shallowing of the lake edge depth and decreased water levels. In contrast, lake shorelines in the eastern region remained relatively stable due to the constructed embankments for the protection of the cultivated farmland. While the seasonal fluctuations of the Tonle Sap Lake are regulated by regional precipitation in the Mekong River Basin, the prolonged shrinking of the lake can be mainly ascribed to intensive anthropogenic activities. The interception of dams along the upper Mekong River has resulted in a decrease in the inflow to Tonle Sap Lake, exacerbating its shrinkage. Moreover, there are minor impacts from

* Corresponding author at: State Key Laboratory of Estuarine and Coastal Research, East China Normal University, Shanghai 200062, China.
E-mail address: zjdai@sklec.ecnu.edu.cn (Z. Dai).

https://doi.org/10.1016/j.scitotenv.2024.170444
Received 22 September 2023; Received in revised form 16 January 2024; Accepted 23 January 2024
Available online 28 January 2024

agricultural land expansion and irrigation on the lake. This study highlights the driving forces behind the evolution of Tonle Sap Lake, providing valuable information for lake managers to develop strategies aimed at conserving and restoring the ecological integrity of the Tonle Sap Lake.

1. Introduction

Lakes, which comprise 87 % of the world's liquid surface fresh water, are vital for ecosystem dynamic equilibrium, climate regulation, and economic development, providing a crucial natural resource for human survival and progress (Peter, 1993; O'Reilly et al., 2015; Woolway et al., 2020). However, lakes worldwide are facing an alarming trend of rapid decline or even complete disappearance, posing a significant threat to local organisms and regional ecosystems (Wurtsbaugh et al., 2017; Knoll et al., 2019). Recent studies indicate that approximately 53 % of the largest global lakes have experienced statistically significant storage declines between 1992 and 2020, attributed to climate change and intensified human activities (Yao et al., 2023). Notable examples include the ongoing 0.8 m/yr decline in the Dead Sea, which has dropped by about 20 m since the early twentieth century (Yechieli et al., 1998). The Aral Sea experienced the most severe destruction, with a 23-m drop in lake level and a 74 % reduction in its area since 1960 (Micklin, 2010). The persistent low water levels and shoreline recession have been observed in the Great Lakes of the United States (Gronewold and Stow, 2014). Poyang Lake, the largest freshwater lake in China, has also experienced a dramatic and prolonged recession (Mei et al., 2015). These alarming trends in lake decline have led to the degradation of the valuable ecosystem services provided by the lakes, including nutrient exchange, carbon cycling, biodiversity promotion, and climate regulation (Adrian et al., 2009; Brönmark and Hansson, 2017; Tao et al., 2015; Mendonça et al., 2017). Consequently, there is a growing global recognition of the need to comprehensively, evaluate the extent of lake decline and identify the underlying driving factors.

Lakes, often referred to as "sentinels of climate change" (Adrian et al., 2009), play a crucial role in integrating basin-scale climatic processes such as precipitation, runoff, and evapotranspiration (Cooley, 2023). The fluctuations of lake water storage are primarily driven by the balance between precipitation and evapotranspiration within a lake's watershed (Woolway et al., 2020). Lakes in tropical regions, including those in western Mexico, Lake Victoria, Lake St Lucia, and Lake Alchichic, have suffered serious impacts from El Niño and La Niña, resulting in abrupt variations in lake areas due to increased or decreased local precipitation (Stager et al., 2007; Alcocer and Lugo, 2003; Humphries et al., 2016; Caballero and Navarro, 2021). With the ongoing global warming, evapotranspiration is increasing, particularly in high-latitude regions, which has direct implications for lakes (Karlsson et al., 2005). A recent study indicated a global average increase in lake evaporation of 3.12 km^3/yr for 1.42 million lakes worldwide (Zhao et al., 2022). Predicted by Wang et al. (2020) suggest a 16 % increase in annual lake evaporation by the end of the century, further accelerating the global trend of lake shrinkage.

Anthropogenic activities also contribute to the fragility of the lake ecosystem (Grant et al., 2021). Uncontrolled land reclamation activities lead to increased sediment deposition in lakes, resulting in a reduction in their size (Du et al., 2011). Furthermore, the impacts of dam construction on lakes have been well-documented, such as the Three Gorges Dam's effects on Poyang Lake and the impacts of hydropower dams on the upper Mekong River Basin (Mei et al., 2015; Dang et al., 2022). As a result, human diversion of water for irrigation further reduces water inputs to lakes, resulting in substantial water loss (Cooley, 2023). Despite the significant changes experienced by many lakes due to climate and human activities, the long-term dynamics of the Tonle Sap Lake in Southeast Asia, the largest lake in the region, has received relatively limited attention.

The Tonle Sap Lake, located on the lower reaches of the Mekong River, serves as a vital habitat for millions of people and faces potential threats from climate changes (Nuorteva et al., 2010; Lauri et al., 2012; Oeurng et al., 2019; Morovati et al., 2023) as well as the pressure from population growth and excessive human activities (Kuenzer, 2014; Lu et al., 2014). It is worth noting that the variability of the Tonle Sap Lake is significantly influenced by the hydrology of the Mekong River (Kummu et al., 2008; Ji et al., 2018b; Morovati et al., 2023), which is, in turn, influenced by large-scale circulations such as the El Niño-Southern Oscillation (ENSO), Pacific Decadal Oscillation (PDO) and Indian Ocean Dipole (IOD) (Räsänen and Kummu, 2013; Chen et al., 2021). Meanwhile, studies have suggested that that precipitation in the Mekong River Basin may also impact variations in the Tonle Sap Lake (Kummu et al., 2008; Delgado et al., 2010; Frappart et al., 2018).

In addition to the impacts of climate change, the development of hydropower operations and irrigation projects in the Mekong River Basin has caused significant alterations to the natural flow regime of the Mekong mainstream Since the 1990s (Cochrane et al., 2014; Chen et al., 2021). Dams located upstream in the Mekong River Basin have the potential to alter the hydrology of the Tonle Sap Floodplain (Wu et al., 2009; Mekong River Commission (MRC), 2011b; Arias et al., 2012). Moreover, recent studies have highlighted the role of local anthropogenic factors, such as riverbed incisions due to sand mining and reduced sedimentation caused by human activities, as significant drivers of hydrological regime changes in the Tonle Sap Lake (Chua et al., 2022; Ng and Park, 2021). Some research suggests that the ecological changes resulting from hydropower development may have more pronounced and severe effects compared to those caused by climate change (Arias, 2013; Lauri et al., 2012). Nevertheless, according to Morovati et al. (2023), as of the early 21st century, human modifications to the Mekong River flow were still minimal. Conversely, recent studies have indicated that variations in precipitation within the Mekong River Basin play a major role in shaping the hydraulic regime, while the impact of dams constructed in China is considered to be inconsequential (Wang et al., 2020; Gu et al., 2021). Consequently, one of the primary concerns, particularly for the Mekong River and the Tonle Sap Lake, is the hydrological alterations resulting from upstream dam construction and the impoundment of reservoirs.

Previous studies have primarily focused on the factors influencing the hydrological aspects of the Tonle Sap Lake, such as lake water balance, water storage, and sediment transport (Kummu et al., 2014; Frappart et al., 2018; Sok et al., 2021; Chen et al., 2021). However, there has been limited research on the spatial elements of the lake and the causes behind their changes. Additionally, the current field observation of lakes provides limited information and has difficulties in capturing large-scale lake changes, let alone providing a comprehensive understanding of the recent dynamics of the Tonle Sap Lake between 2000 and 2020. In recent decades, the advancement of remote sensing technology, along with sophisticated classification algorithms and image processing techniques, has it easier to map lakes at a larger scale (Gu et al., 2021). Medium-resolution satellite images, such as Moderate Resolution Imaging Spectroradiometer (MODIS) and Land Remote Sensing Satellite (Landsat) images have been widely utilized for lake mapping (Zhou et al., 2019; Ji et al., 2018a). Therefore, by employing a comprehensive methodology that combines remote sensing images with field observations of the Tonle Sap Lake, the main objectives of this study were to (1) investigate the interannual and intra-annual hydrological dynamics of the Tonle Sap Lake; (2) map morphological changes of the lake, and (3) identify the possible driving forces behind the lake dynamics. This research aims to provide crucial insights contributing to the sustainability of lakes in Southeast Asia and establish a foundation for

managing risks in global lakes, as they respond to similar environmental impacts.

2. Materials and methods

2.1. Study area

The Tonle Sap Lake is located in the downstream plain of the Mekong River. As the largest freshwater lake in Southeast Asia, it spans a total watershed area of 81,663 km^2 [Lat. 11–15°N, Long. 102–106°E] (Fig. 1). The Tonle Sap Lake holds significant importance as the fourth-largest inland fishery production in the world, accounting for over 70 % of Cambodia's annual inland fishery catch and supporting the livelihoods of eight million people in the surrounding areas (Morovati et al., 2023; Arias et al., 2012; Kummu et al., 2008; Campbell et al., 2006). The Tonle Sap Lake is influenced by a tropical monsoon climate, characterized by a flood season from May to October and a dry season from November to April (Siev et al., 2016). It acts as a natural reservoir along the Mekong River, accumulating and storing water during the peak flooding season to mitigate downstream flooding. Subsequently, it releases water during the dry season, sustaining its ecological environment (Kummu et al., 2014). This process is referred to as the "flood pulse" (Junk et al., 1989; Kummu et al., 2008). The connection between Tonle Sap Lake and the Mekong River is established through the Tonle Sap River, and is highly sensitive to the flood pulse and flow variations of the Mekong River (Lee et al., 2021). Water inflow into the Tonle Sap Lake originates from three main sources: the mainstream of the Mekong River (53.5 %), its tributaries (34 %), and direct precipitation (12.5 %). Conversely, the water outflow from the Tonle Sap Lake primarily occurs through two main channels: direct evaporation and outflow to the Tonle Sap River (Kummu et al., 2014).

2.2. Materials

Google Earth Engine (GEE) is a powerful tool for analyzing geospatial data on a planetary. It integrates a vast catalog of satellite imagery including Landsat surface reflectance data processed by the United States Geological Survey (USGS) (https://earthexplorer.usgs.gov) (Long et al., 2022). For the analysis of long-term area changes of the Tonle Sap Lake, multiple remote sensing images from MODIS are used as the primary data sources. The spatial changes of the Tonle Sap Lake are determined using Landsat imagery between 2000 and 2020. Additionally, the daily water level of the Tonle Sap Lake at Kampong Loung station and the daily discharge of the Mekong River at Kratie station can be available from the Mekong River Commission data portal (https://portal.mrcmekong.org/time-series). Additionally, the monthly precipitation data for the Tonle Sap Lake basin and Mekong River Basin (from 2000 to 2019) are obtained from the Tropical Rainfall Measuring Mission (TRMM) 3B43 Version 7 dataset known for its accuracy rate surpassing 95 % (Zhang et al., 2019; Wang and Lu, 2015), available at https://disc.gsfc.nasa.gov/datasets/TRMM_3B43_7/summary. Furthermore, the monthly evaporation volume for the Tonle Sap Lake basin is obtained from the Global Lake Evaporation Volume (GLEV) dataset with an accuracy rate of 91.52 % (Zhao et al., 2022), accessible at https://zeternity.users.earthengine.app/view/glev on GEE platform. Moreover, the total installed capacity and number of dams in the upper Mekong River region were taken from the Open Development Mekong, dating back to the year 2000 (Open Development Mekong (ODM), 2021).

2.3. Methods

2.3.1. Image processing

The extracting surface area of the Tonle Sap Lake is based on two MODIS datasets, MODIS/006/MOD09A1 and MODIS/006/MOD44W. Integrating the two datasets into monthly median composites to obtain clear composites and avoid the influence of sensor noise, clouds, or

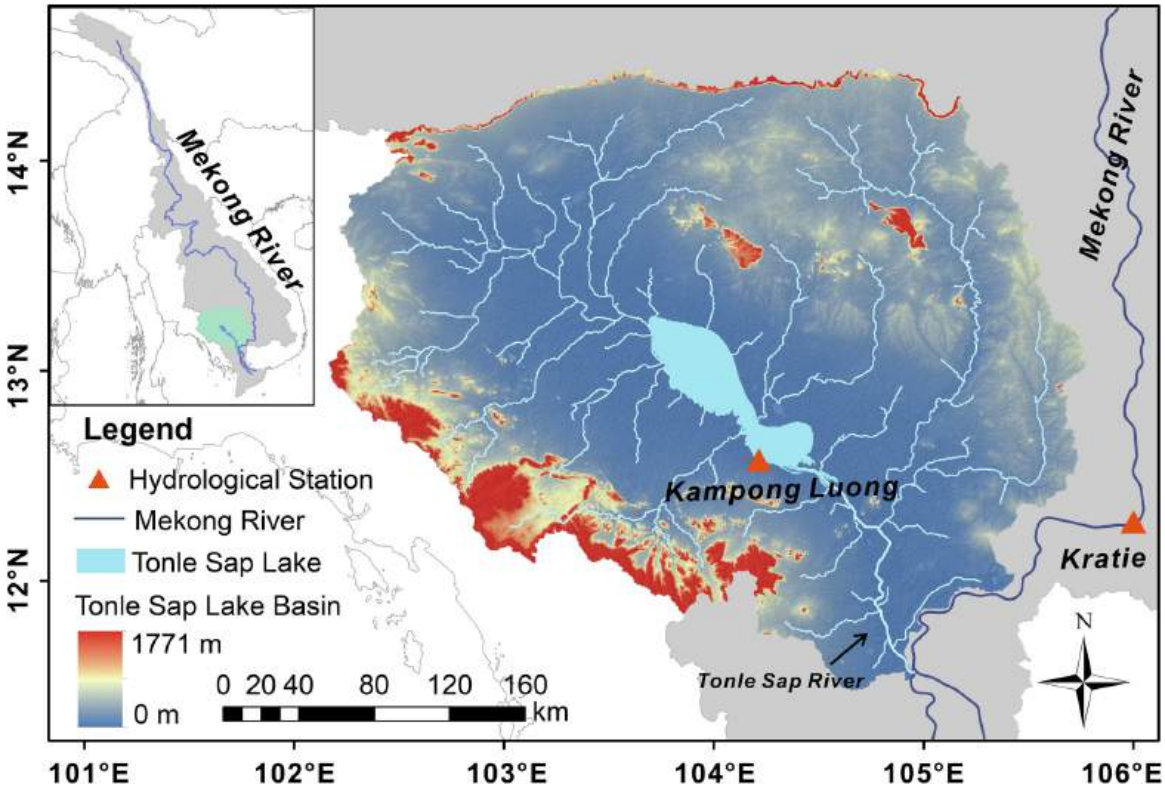

Fig. 1. Location map of the Tonle Sap Lake basin, including distribution of hydrological stations.

cloud shadows. A combination of visual and shortwave infrared bands was applied with the method proposed by Ji et al. (2018a) to perform an optical-based monthly open-water area extraction. If a pixel meets either of the following two conditions outlined in Table 1, it is classified as water:

Surface reflectance data from Landsat Thematic Mapper (TM)/ Enhanced Thematic Mapper Plus (ETM+)/Operational Land Imager (OLI), provided by the GEE, are utilized to identify lake shorelines of the Tonle Sap Lake from 2000 to 2020 with higher accuracy. Given the vast lake area, images with cloud cover below 40 % are initially screened. The CFmask function is employed to eliminate clouds and snow from each image, which is a tool designed to generate masks for cloud, shadow, and snow cover in remote sensing imagery (Foga et al., 2017). Subsequently, high-quality image sets without clouds, snow, and terrain shadow are generated using digital elevation models. The remaining pixels in the image sets are considered good quality Landsat observations suitable for mapping surface water bodies. Finally, annual collections of cloud- and snow-free images are created for each year from 2000 to 2020 based on Landsat TM, ETM+, and OLI images within the study area using GEE (Nyland et al., 2018). Fig. 2 displays the annual total number of Landsat satellite images. A threshold-based method proposed by Zhou et al. (2019) is employed to extract water bodies from the generated image collections, by utilizing multiple water indices such as MNDWI, NDVI, and EVI for identification. In this approach, water bodies are identified by classifying pixels that satisfy the conditions (MNDWI > NDVI or MNDWI > EVI) and (EVI < 0.1) as water. These spectral indices are calculated based on Table 2, where ρRed, ρGreen, ρBlue, ρSwir 1, and ρNir are the reflectance values of red, green, blue, shortwave infrared, and near-infrared bands, respectively. Furthermore, pixels that satisfy the threshold requirements are identified as water bodies and assigned a value of 1. Otherwise, they are assigned a value of 0. The

Table 1
Rule-Based water classification.

	Condition	Equation
1	High-reflectance water	$maxVIS \geq T_{VIS} \&\& WI = 1 \&\& maxSWIR < T_{SWIR} = 0.1$
2	Low-reflectance water	$maxVIS < T_{VIS} \&\& maxSWIR < T_{SWIR} \&\& NDVI < T_{NDVI} = 0.2$

Where $T_{VIS} = 0.05$, $maxVIS = max\,(\text{Band1}, \text{Band2}, \text{Band3})$,$maxSWIR = max\,(\text{Band6}, \text{Band7})$, and Bands 1–7 correspond to the specific spectral bands sur_refl_b01–07 in the MODIS/061/MOD09A1 product. If $maxVIS \leq maxSWIR$, the Water Index (WI) is 0; otherwise, WI is 1. Moreover, $NDVI = \frac{\text{Band4} - \text{Band3}}{\text{Band4} + \text{Band3}}$. Subsequently, the Condition 1 and Condition 2 images are integrated, with the pixel bearing the highest value chosen from this image collection, effectively amalgamating the two images. The resulting image is then multiplied by the area of an individual pixel (0.25 km^2), ultimately providing the measurement for the surface area of the lake. Due to the absence of mountains and hot weather conditions, along with the use of monthly mosaic images that are cloud-free, there is no need for object-based post-classification. This approach helps avoid misrecognizing water as clouds or ice/snow flags. The accuracy of extracting water that is easily misrecognized is reported to be over 93 % (Ji et al., 2018a, 2018b). As this study utilizes remote sensing to detect the long-term surface area variations in the Tonle Sap Lake, there are inevitable data source errors from MODIS images which primarily refers to the pixel error of 0.25km^2, resulting from the 500 m spatial resolution of MODIS images. To mitigate this error, selecting a large-scale study object such as Tonle Sap Lake with a surface area ranging from 2000 km^2 to 15,000 km^2, is crucial to ensure the reliability of results (Okin and Gu, 2015). The proportion of pixel error to the minimum lake area is <0.02 %, suggesting a negligible impact of pixel error on the calculation of lake area. Finally, the monthly surface area measurements for Tonle Sap Lake from 2000 to 2020 are compared with previous research findings by Gu et al. (2021), Wang et al. (2020), and Frappart et al. (2018). This comparison reveals a high degree of consistency between the results obtained in this study and the findings of the previous research.

water frequency in a given year is calculated for all pixels in the basin using the following formula:

$$F(y) = \frac{1}{N_y} \sum_{i=1}^{N_y} w_{y,i} \times 100\% \quad (1)$$

where F is the water frequency of the pixel, y is the specified year, N_y refers to the total number of high-quality observations of that pixel in the given year, and $w_{y,i}$ represents whether an observation value of the pixel is water or not, with 1 indicating water and 0 indicating non-water. Annual water frequency maps of the Tonle Sap Lake were generated by the annual frequencies of all Landsat pixels. After setting a certain threshold, the water body areas are derived from the annual water frequency maps, and they vary according to different threshold values. We compared the water body areas of the Tonle Sap Lake using different frequency thresholds with annual minimum areas extracted from MODIS and found a good agreement between the two datasets when the frequency threshold of our datasets was set to 0.90. Therefore, water bodies exceeding the 90 % threshold are employed for annual shoreline extraction.

2.3.2. Digital shoreline analysis system (DSAS)

The DSAS, an automated software extension for ArcGIS (Lou et al., 2022) (https://code.usgs.gov/cch/dsas), was used in this study to analyze the historical shoreline changes of the Tonle Sap Lake and to quantify the lake' shrinking. Specifically, the shoreline in 2000 was defined as the baseline, which was divided into 347 segments, each with a distance of 1000 m. To track shoreline changes over time, one shoreline was chosen for calculation every five years from 2000 to 2020. Then, the DSAS automatically generated the interannual edge line migration for each transect. Based on the endpoint rate, the transects were divided into three segments: transects 1 to 160 were designated as S_1, transects 161 to 260 as S_2, and transects 261 to 347 as S_3. These segment divisions allow for a more detailed analysis of shoreline changes in different areas of the Tonle Sap Lake over the study period.

2.3.3. Mann-Kendall test

In this study, the Mann-Kendall (MK) test is employed as a non-parametric statistical analysis approach to assess the statistical monotonic trends and change patterns in two sets of time series data: monthly average water levels of the Tonle Sap Lake (Tonle Sap Lake) from January 2000 to December 2020, and Mekong River discharge data at the Kratie station during the same period. The MK test is chosen for its computational simplicity and independence from specific distribution requirements. It is robust against outliers and widely used by researchers to analyze trends in various sequences, including temperature, precipitation, water quality, and more (Wei, 1999). The MK test involves calculating two statistics: UF (forward sequence) and UB (reverse sequence), which represent the changing trend of the time series. Specifically, a positive value of UF indicates an upward trend in the original statistical series, while a negative value suggests a downward trend. The absolute value of UF is compared to a critical value of 1.96 to determine whether the trend is statistically significant at a significance level of $\alpha = 0.05$. During change point analysis, two sets of statistical variables are calculated: one in the forward sequence, UF_k, and the other in the reverse sequence, UB_k. If the UF_k and UB_k curves intersect, and the intersection point falls between the critical lines (between ±1.96), it can be inferred that the point of intersection corresponds to the time when an abrupt change occurred (Gao et al., 2015). By applying the MK test to the monthly average water levels of the Tonle Sap Lake and Mekong River discharge data, the study aims to identify any significant trends or change points in these variables over the specified period.

2.3.4. Water level analysis

According to Intergovernmental Panel on Climate Change (IPCC) (2007), extreme hydrological events can be classified based on specific

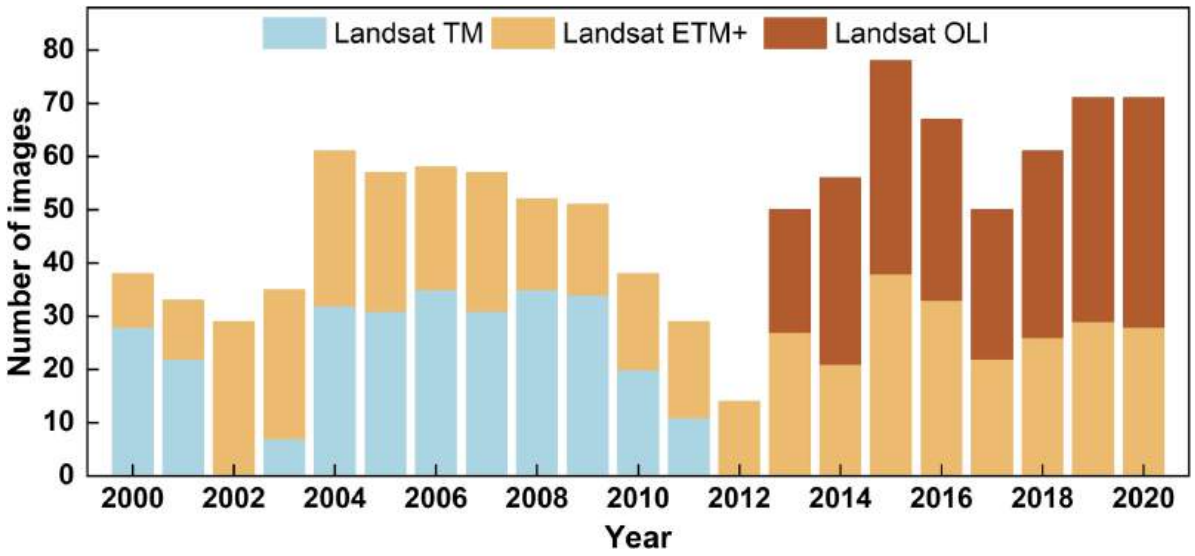

Fig. 2. The total number of satellite images.

Table 2
Spectral indices used for extracting water.

	Name	Equation	References
1	Normalized Difference Vegetation Index (NDVI)	$NDVI = \frac{\rho Nir - \rho Red}{\rho Nir + \rho Red}$	Rouse et al., 1974
2	Enhanced Vegetation Index (EVI)	$EVI = 2.5 \times \frac{\rho Nir - \rho Red}{\rho Nir + 6\rho Red - 7.5\rho Blue + 1}$	Huete et al., 2002
3	Modified Normalized Difference Water Index (MNDWI)	$MNDWI = \frac{\rho Green - \rho Swir1}{\rho Green + \rho Swir1}$	Xu, 2006

thresholds derived from the distribution of climate or weather variables. In this study, the threshold for identifying flood water levels is set at the 90th percentile, which corresponds to values greater than the 8-m mark. To calculate the percentile values for the monthly water levels between 2000 and 2020, the methodology outlined in Bonsal et al. (2001) is followed. Series of monthly water levels are first ranked in an ascending order $Q_1, Q_2, \ldots, Q_m$, and the probability p that a random monthly water level is less or equivalent to the rank of the Q_n is calculated by the formula as follows:

$$p = \frac{n - 0.31}{m + 0.38} \quad (2)$$

where m denotes the total number of daily water levels contained in the series and n represents the rank of the water level at the desired percentile.

Moreover, in examining the repercussions of human activities across various temporal phases within the Mekong River basin, this study employs dam-related data to evaluate the intensity of such activities. Illustrated in Fig. 3, the period preceding 2007 witnessed a relatively low count of dams and a modest total installed capacity. However, a discernible surge in both the number of dams and total installed capacity is evident post-2014. Furthermore, to enhance comparability throughout the research timeframe spanning from 2000 to 2020, we have partitioned it into three distinct stages: 2000–2006, 2007–2013, and 2014–2020.

3. Results

3.1. Water level changes of the Tonle Sap Lake

The water level of the Tonle Sap Lake has shown a substantial and statistically significant declining trend since 2000, with a significance

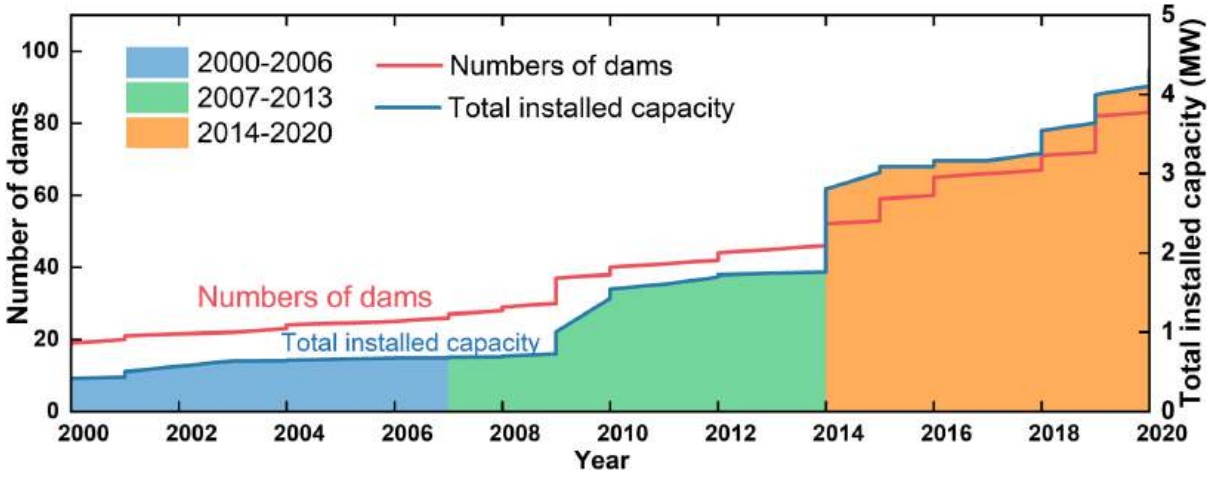

Fig. 3. Historical increase in the number of dams and their total storage volume.

level of 0.005, and this decline is accompanied by noticeable seasonal variations (Fig. 4A). The monthly average water levels were 4.35 m, 3.87 m, and 2.99 m for the first, second, and third stages, respectively. Comparing these stages, there was a decrease in water level of 0.48 m between the first and second stages and a further decrease of 1.36 m between the first and third stages (Fig. 4A). Additionally, the Mann-Kendall test reveals both an annual variation trend and an abrupt change in the water level of the Tonle Sap Lake. The test statistic UF_k has consistently remained below 0 since 2003, indicating a continuous decline in water levels. The intersection of UF_k and UB_k within the 0.05 significance level confidence interval around 2013, signifies a notable abrupt change (Fig. 4B).

Furthermore, across the three stages, the proportion of low water levels continues to increase, while the proportion of high water levels steadily decreases (Fig. 5A). Additionally, the duration exceeding the extreme flood level of 8 m decreased from 51 days in the first stage to 24 days in the second stage. In the third stage, the highest water level did not even surpass 7 m (Fig. 5B). Consequently, both the second and third stages exhibited a delayed onset and early cessation of the flood season compared to the first period (Fig. 5B). Notably, the rates of water level rise from the onset of the flood season (May 1st) to the annual peak water level for these three stages were 1.49 m/month, 1.30 m m/month, and 1.03 m/month, respectively (Fig. 5B). Taken altogether, the monthly average water level exhibited a significant decline from the first stage to the third stage in both the flood season and the dry season. The water level of Tonle Sap Lake demonstrates a characteristic of no flooding in the flood season and the dry season is getting drier.

3.2. Area changes of the Tonle Sap Lake

The surface area of the Tonle Sap Lake displays significant seasonal fluctuations at the monthly scale, characterized by a nadir observed between April and June, and a peak typically recorded in September or October (Fig. 5). However, the surface area of the lake has also undergone distinct phases of transformation. In contrast to the first phase, where the mean monthly surface area measured 5635 km^2, the subsequent period indicated a marginally diminished expanse of 5475 km^2. However, the subsequent phase exhibited a more pronounced shrinking, measuring 4678 km^2 (Fig. 6). Concurrently, a notable reduction in the annual mean surface area of the lake has been observed, demonstrating

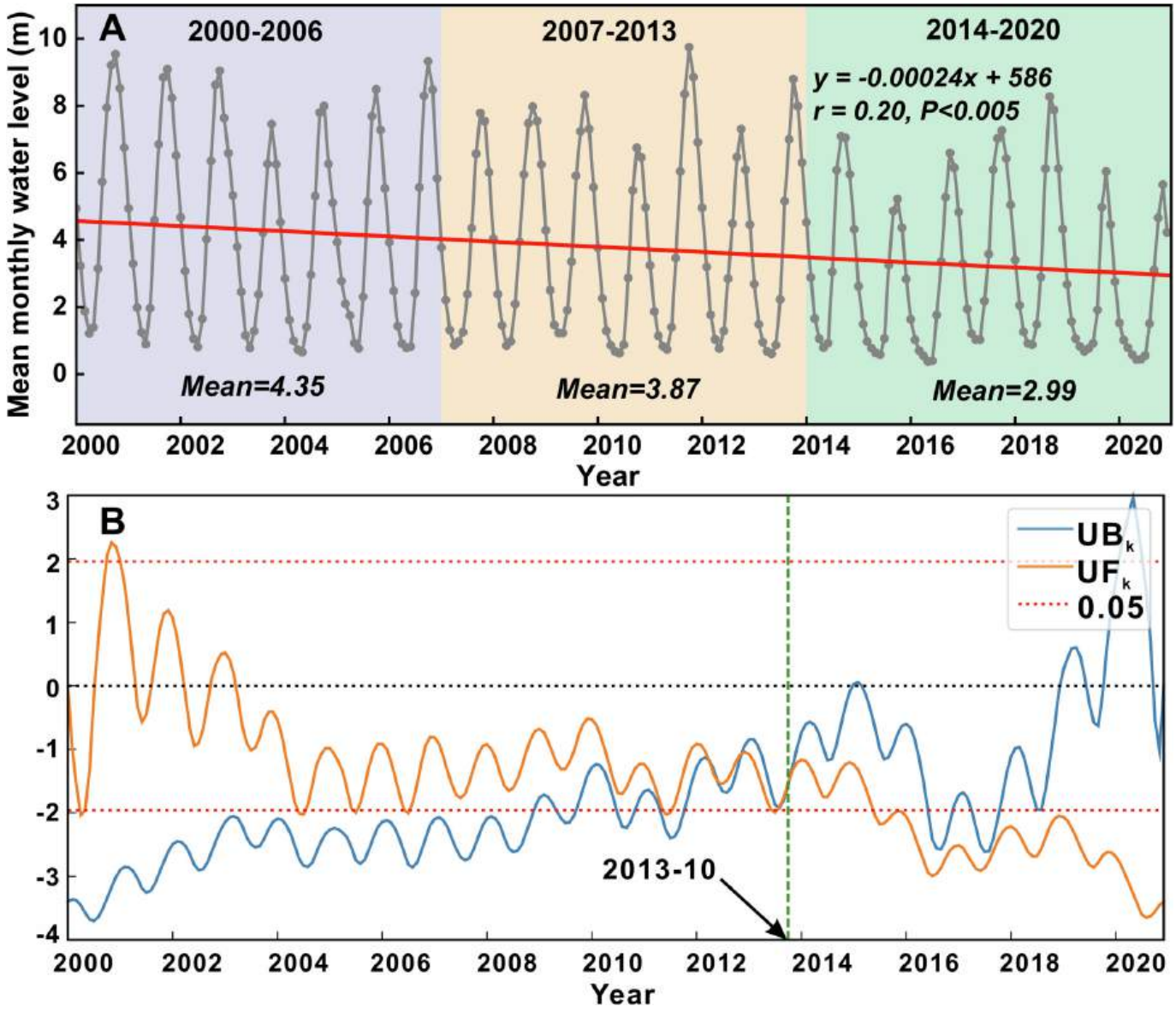

Fig. 4. A: Mean monthly water level of the Tonle Sap Lake between 2000/01 and 2020/12; B: The Mann-Kendall test of water level of the Tonle Sap Lake between 2000 and 2020.

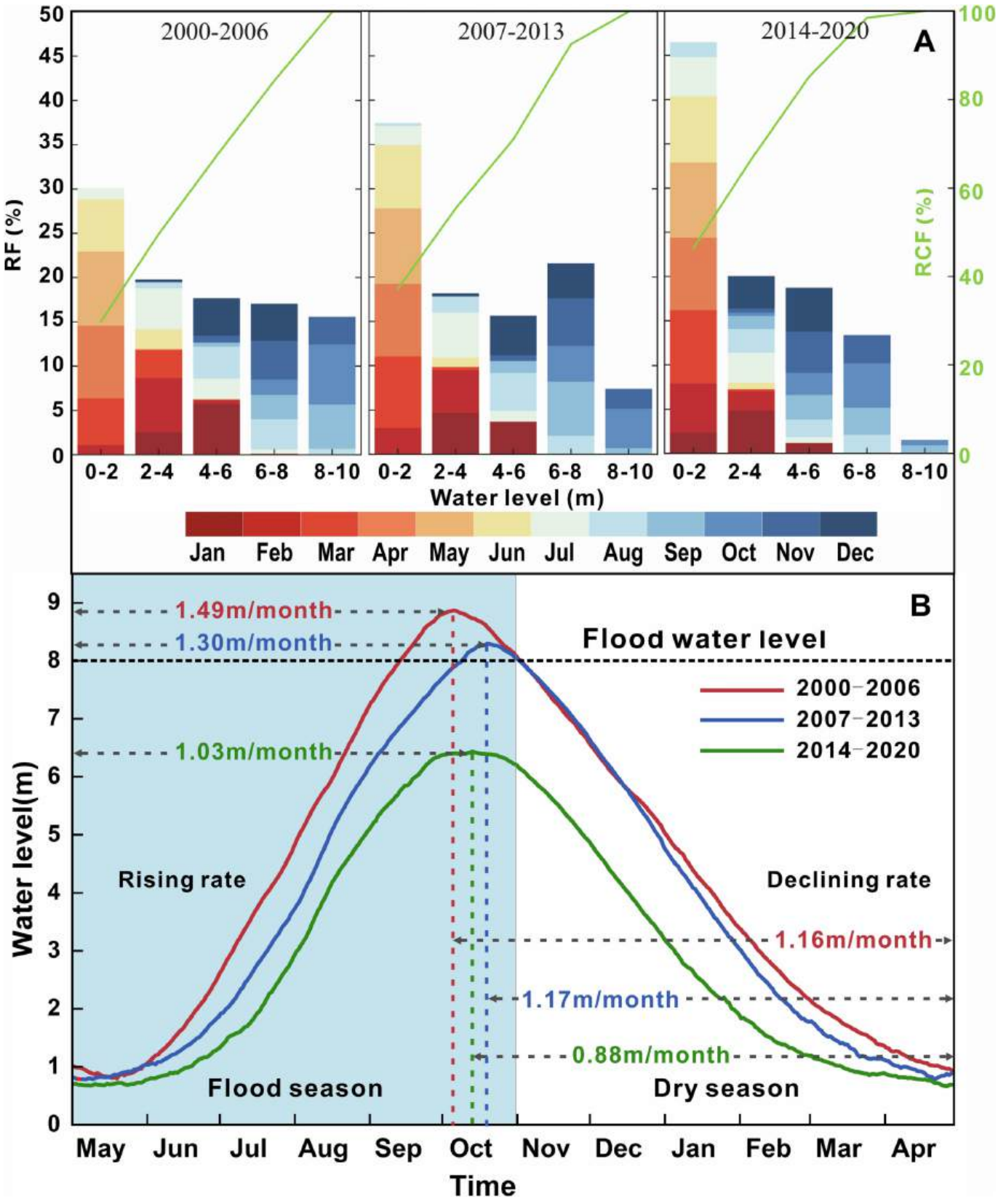

Fig. 5. A: Different stages of water level in the Tonle Sap Lake between 2000 and 2020; B: Average water level and water level rise/decline rate of different periods.

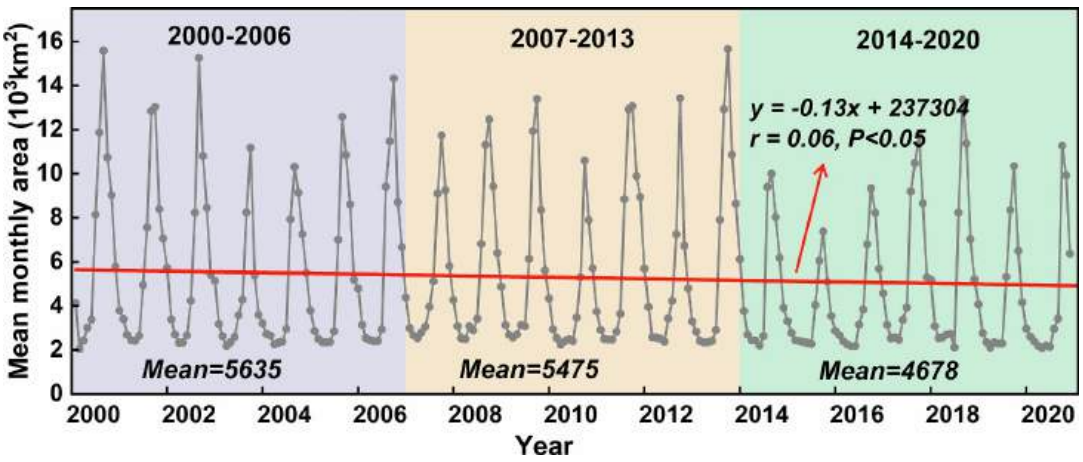

Fig. 6. Average monthly surface area of the Tonle Sap Lake between 2000/02 and 2020/12.

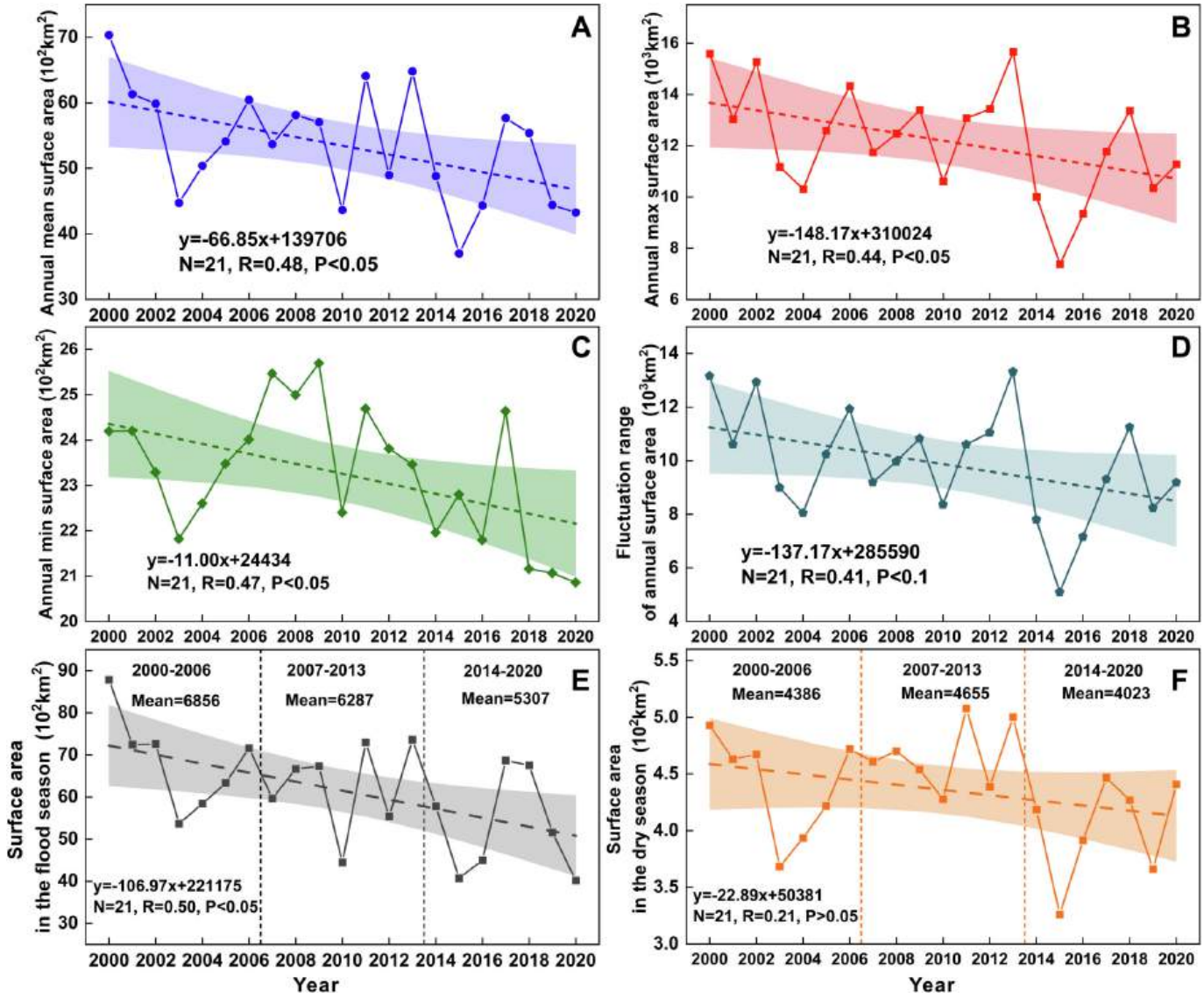

Fig. 7. Surface area variations of the Tonle Sap Lake from 2000 to 2020. A: Annual mean surface area; B: Annual max surface area; C: Annual min surface area; D: Fluctuation range of annual surface area; E: Lake surface area of flood season; F: Lake surface area of dry season.

a substantial decline at a rate of 66.85 km^2/yr (Fig. 7A). The annual peak surface area of the lake displays an exceptionally steep descent, declining at a rate of 148.17 km^2/yr (Fig. 7B). As the intensity of flooding diminishes, the annual flood extent shrinks, indicating that certain areas of the floodplains are no longer inundated during the wet season. Simultaneously, the annual minimum surface area presents a conspicuous reduction at a rate of 11.00 km^2/yr (Fig. 7C), highlighting increased land exposure during dry periods. Notably, the annual fluctuation range of surface area is diminishing at a rate of 137.17 km^2/yr (Fig. 7D), indicating a discernible weakening in the Tonle Sap Lake's flood pulse dynamics. During the flood season, the lake has experienced a substantial decrease at a rate of 106.97 km^2/yr, and it decreased from 6856 km^2 in the first period to 6287 km^2 in the second period and further decreased to 5307 km^2 (Fig. 7E). However, during the dry season, while the lake's extent diminishes at a rate of 22.89 km^2/yr, there is a slight increase in the second period (Fig. 7F). In brief, the span from 2000 to 2020 has witnessed a pronounced contraction in the Tonle Sap Lake, accompanied by a substantial reduction in flood pulses and notable shrinkages during the flood season. Simultaneously, the dry season has displayed a trend of a non-significant decline.

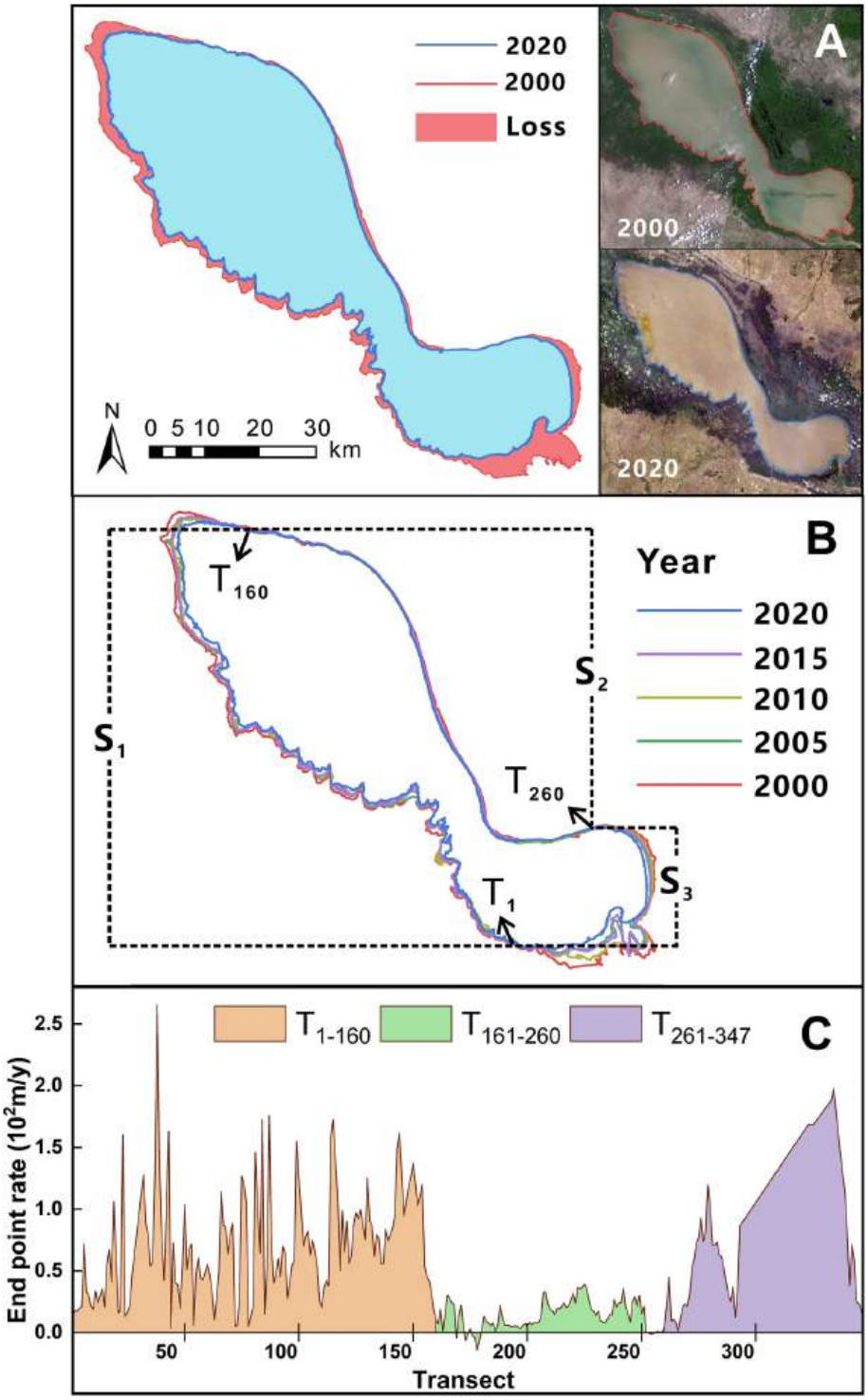

Fig. 8. A: Lake shoreline of 2000 and 2020; B: Lake shoreline of from 2000 to 2020; C: End point rate of S_1, S_2 and S_3 from 2000 to 2020 (T_1 represents transect 1).

3.3. Lake shoreline changes

The Tonle Sap Lake has undergone a significant decrease in its dry season total open water area over the past two decades (Fig. 8A, B). In the year 2000, the lake had an approximate area of 2419 km^2, which diminished to 2086 km^2 by 2020, representing a decline of 13.8 % (Fig. 8A). While it is important to note that 2000 experienced a flood year while 2020 was a drought year. However, based on the lake's historical shorelines, the ongoing shrinking of the lake is evident. The western part of the lake has experienced pronounced shrinkage, as has the southeastern part of the lake, where the Tonle Sap River meets the Tonle Sap Lake at its inlet. In contrast, the eastern part of the lake has not exhibited conspicuous shrinking, with the shorelines from several years overlapping consistently (Fig. 8B). The entire lake exhibits an average shoreline shrinking rate of 47 m/yr. The shrinking of S_1 shows significant fluctuations in its rate, with an average annual recession rate of 68 m, accompanied by a highly irregular shoreline. On the other hand, S_2 exhibits a recession rate of 13 m/yr, accompanied by a straight and smooth shoreline. Positioned at the lake's inlet, S_3 is shrinking at a rate of 61 m/yr (Fig. 8C). Moreover, we have observed that the declining trend observed in the average water levels during the driest three months (April to June) of the years 2000, 2005, 2010, 2015, and 2020-measuring 1.91 m, 1.14 m, 0.73 m, 0.67 m, and 0.49 m, respectively.

4. Discussion

4.1. Impacts from climatic changes

Climate change has consistently been identified as the pivotal factor influencing the rapid fluctuations in lakes (Adrian et al., 2009). Climate change directly affects regional precipitation patterns, resulting in either increased or decreased levels of regional precipitation (Dore, 2005; Xiao

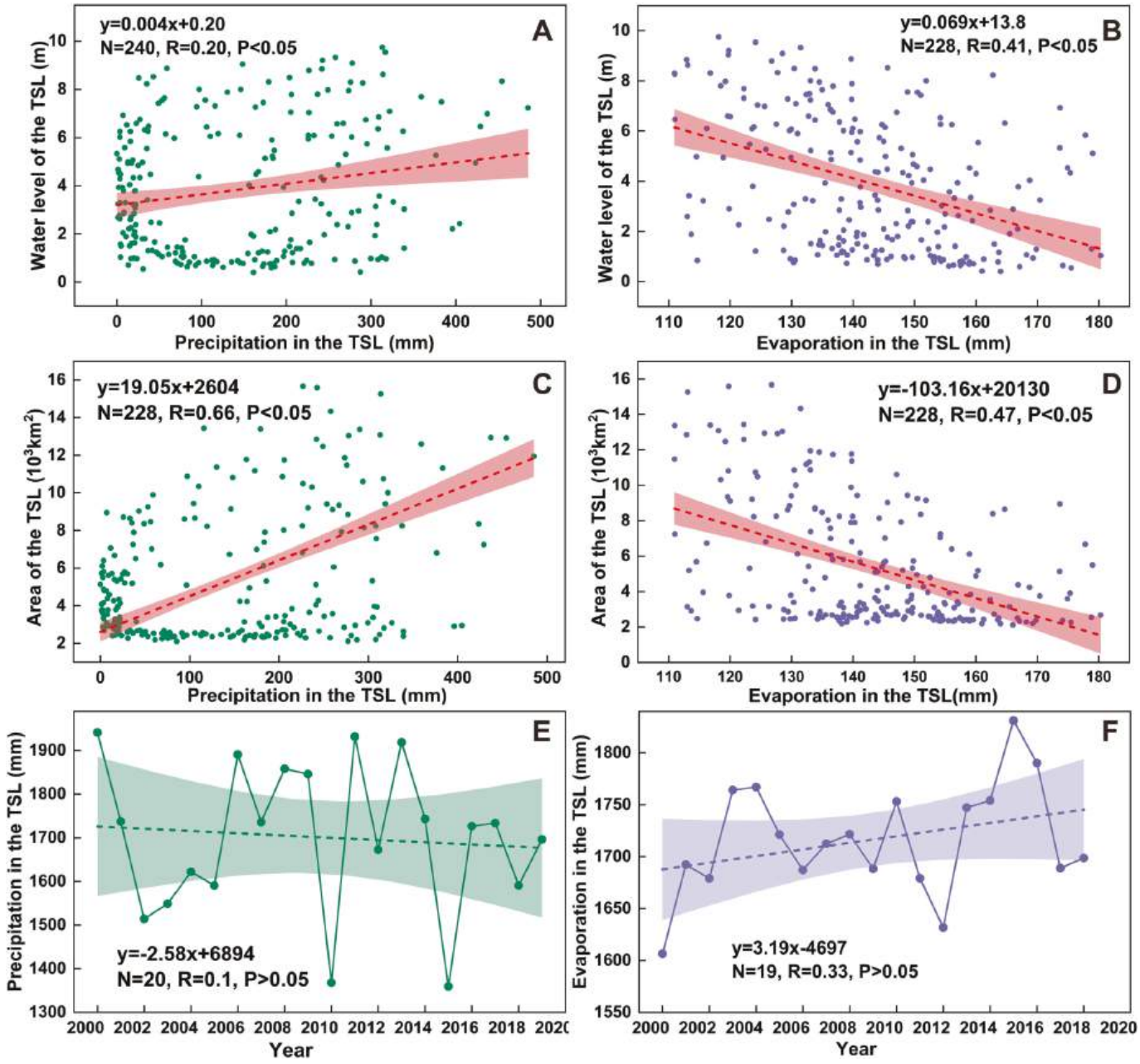

Fig. 9. A-D: Correlations between the monthly mean water level/surface area of the Tonle Sap Lake (TSL) and the precipitation and evaporation in the Tonle Sap Lake basin; E and F: Long-term annual mean precipitation and evaporation from 2000 to 2019/2018 in the Tonle Sap Lake basin.

et al., 2015). While previous research has extensively investigated the cumulative impact of precipitation on surface water storage in the Tonle Sap Lake, including the manifestation of severe droughts and floods (Frappart et al., 2018; Wang et al., 2020), there exists a gap in our understanding of the intricate impact of rainfall and evaporation on the dynamics of the Tonle Sap Lake at seasonal and interannual scales. In this study, we investigated the intricate relationship between rainfall, evaporation, and the dynamics of the Tonle Sap Lake. The weak/significant correlations were observed between the monthly mean water level/surface area of the Tonle Sap Lake and monthly mean precipitation in the Tonle Sap Lake basin ($R = 0.20/R = 0.66$) (Fig. 9A, C), suggesting precipitation plays a dominant role in shaping the intra-annual variation of the Tonle Sap Lake due to climate fluctuations. Meanwhile, the monthly mean water level/surface area of the Tonle Sap Lake exhibits a notably strong negative correlation with the evaporation in the Tonle Sap Lake basin ($R = 0.41/R = 0.47$) (Fig. 9B, D), indicating that the increase in evaporation resulting from climate fluctuations serves as the driving force behind the intra-annual changes in the lake. However, our study indicates that annual precipitation and evaporation in the Tonle Sap Lake basin have not exhibited distinct trends (Fig. 9E, F), indicating that neither rainfall nor evaporation can solely account for the long-term fluctuations in water level and surface area of the Tonle Sap Lake. Notably, the water level and surface area of the Tonle Sap Lake have consistently declined over the past two decades (Fig. 4A, Fig. 6).

Furthermore, we conducted an in-depth examination of the relationship between precipitation in the entire Mekong River basin and

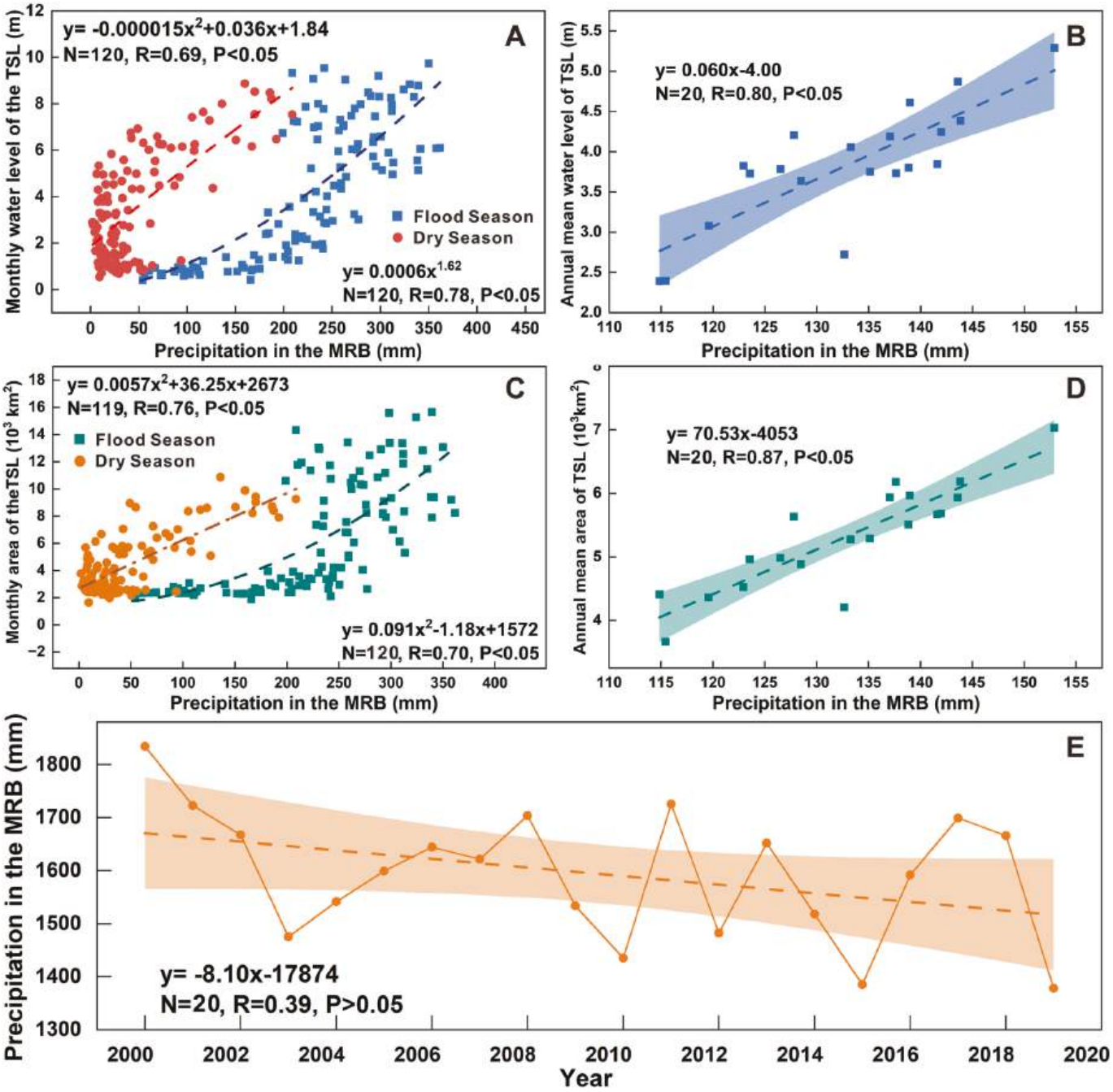

Fig. 10. A/C: Correlations between the monthly mean water level/surface area of the Tonle Sap Lake (TSL) and the precipitation in the Mekong River basin (MRB); B/D: Correlations between the annual mean water level/surface area of the Tonle Sap Lake and the precipitation in the Mekong River basin; E: Long-term annual mean precipitation from 2000 to 2019 in the Mekong River basin.

changes in the lake. The results reveal significant correlations between the monthly mean surface area/water level and monthly mean precipitation in the entire Mekong River basin (Fig. 10A, C), as well as between the yearly mean surface area/water level and yearly mean precipitation in the entire Mekong River basin ($R = 0.87$/R = 0.8) (Fig. 10B, D). Previous studies have also emphasized the significant influence of rainfall on long-term variations in water discharge in the Mekong River basin (Tang et al., 2023). Our observations further revealed a decline in annual rainfall in the Mekong River (Fig. 10E), and similar findings have also been corroborated in earlier studies using different datasets (Wang et al., 2020; Wu et al., 2016). Additionally, previous studies have demonstrated that climate change has impacted the lake dynamics (Morovati et al., 2023). As a result, the recent shrinkage of the Tonle Sap Lake can likely be attributed to reduced runoff resulting from reduced precipitation in the Mekong River basin. In other words, precipitation across the entire Mekong River basin regulates the flow of the Mekong River, which in turn drives both intra-annual and interannual variations in the Tonle Sap Lake.

4.2. Impacts from riverine flow and suspended sediment discharge

The classical river-connected drain lakes are highly influenced by their riverine environments (Yin et al., 2007; Mei et al., 2015). In the case of the Tonle Sap Lake, during the reverse flow period from May to October, >44 % of the total lake inflow to the Tonle Sap Lake is derived from the Mekong River (Kummu et al., 2008; Arias et al., 2012; Dang et al., 2022). Previous studies have reported a decreasing trend in water discharge into the lake (Dang et al., 2022; Chua et al., 2022; Tang et al., 2023). However, the specific impact of changes in Mekong River runoff on the Tonle Sap Lake is still unknown. Therefore, we investigated the relationship between Mekong River runoff and changes in the Tonle Sap Lake. Our analysis reveals a significant declining trend ($R = 0.52$) in the annual mean runoff of the Mekong River, with an average annual decrease of nearly 200 m^3/s (Fig. 11A). Furthermore, a robust correlation is observed between the runoff of the Mekong River in the preceding month and the water level/surface area of the Tonle Sap Lake, with correlation coefficients of 0.93 and 0.99, respectively (Fig. 11B, C). This result explicitly suggests that changes in mainstream discharge primarily drive the changes in surface area and water level change of the Tonle Sap Lake, a phenomenon also observed in Poyang Lake (Li et al., 2017; Tian et al., 2023). Furthermore, a notable shift in Mekong River runoff occurred in July 2013, directly influencing a subsequent abrupt alteration in the water level of the Tonle Sap Lake in October 2013 (Fig. 11D, Fig. 4). The observed time lag between these events suggests a cause-and-effect relationship between the Mekong River runoff and Tonle Sap Lake water level. Therefore, changes in Mekong River runoff changes may be responsible for the long-term recession of the Tonle Sap Lake.

Regarding suspended sediment discharge, an average of 5.7×10^9 kg of total suspended sediment was stored in the lake and its floodplain from 1997 to 2003, primarily accumulating at the lake's edge and in the floodplain (Kummu et al., 2008). If the sediment were to settle out in the permanent lake, it would contribute to a layer of approximately 1.42 mm thick each year. Alternatively, if it settle out evenly over the entire lake and floodplain area, the layer would be approximately 0.27 mm thick each year. Penny et al. (2005) and Tsukawaki (1997) have shown that the net sedimentation rate in the north-western part of Tonle Sap Lake has averaged 0.1 mm/year, and in the north-eastern part, it has been 0.16 mm/year for the past 5500 years B.P. until now. Hence, sediment accumulation would not be the driving factor of the variation behind the Tonle Sap Lake's dimensions. However, the sediment contributes to localized erosion and sedimentation issues (Kummu et al., 2008), and could be a reason for the uneven shrinking of the Tonle Sap Lake. Our findings suggest that changes in Mekong River runoff are likely responsible for the long-term recession of the Tonle Sap Lake, while sediment accumulation does not appear to be a significant driving factor.

4.3. Dams impacts from upstream

The interception of runoff by river dams has been shown to reduce the inflow of water into lakes, a phenomenon that has been observed in various lakes (Zhang et al., 2012; Dang et al., 2022). In the case of the Tonle Sap Lake, we present information regarding the number and total

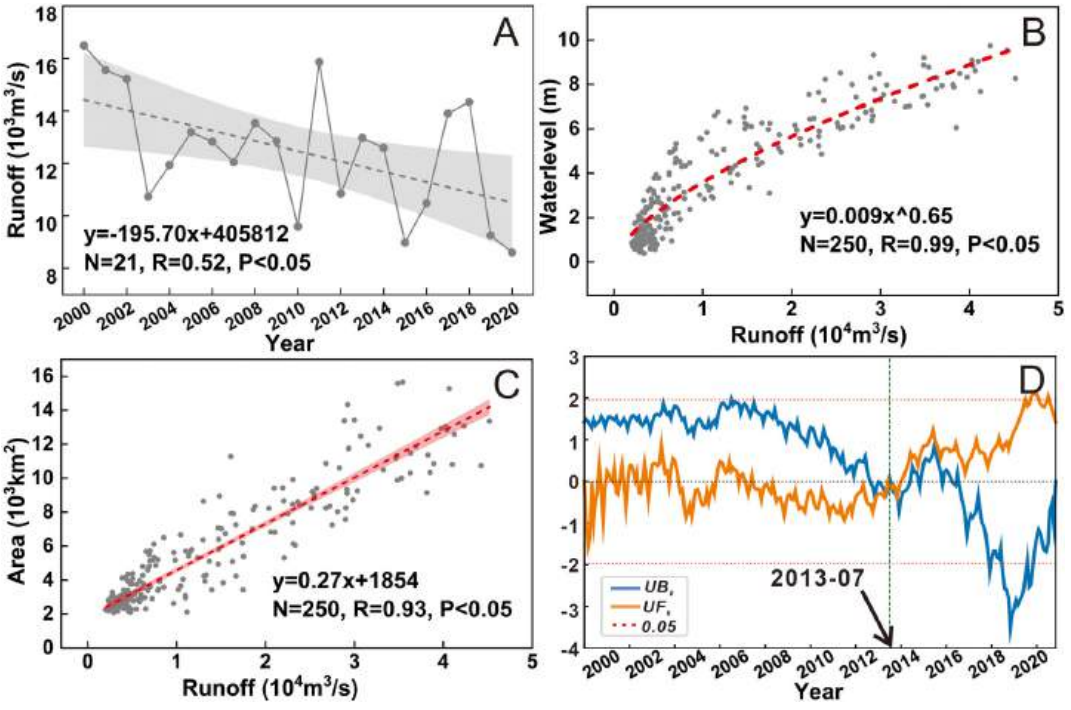

Fig. 11. A: Long-term annual mean runoff at Kratie station from 2000 to 2020; B/C: Correlations between the previous month's Mekong River runoff and water level/surface area of the Tonle Sap Lake; D: The Mann-Kendall test of runoff of Mekong River at Kratie station between 2000 and 2020.

installed capacity of dams located upstream of the Mekong River, which contribute to the inflow of the Tonle Sap Lake (Fig. 3). In the first period, the number and capacity of dams along the Mekong River remained at a relatively low level, and the flow regime of the Mekong River remained largely unchanged with minimal human interference (Mekong River Commission (MRC), 2005; Morovati et al., 2023). Then, there was a significant increase in both the number and capacity of dams, marked by a spike around 2014, with the operationalization of several large dams within China, particularly Nuozhadu, leading to a substantial alteration in the hydraulic regime of the Mekong River Basin (Eyler, 2020). This increase in dam construction coincided with a sudden decrease in Mekong River runoff in 2014 (Fig. 11D), which could have a further impact on the Tonle Sap Lake (Fig. 4B). The continued construction of dams after 2014 further disrupted the hydraulic regime, resulting in reduced Mekong River discharge and subsequent contraction of the Tonle Sap Lake. Consequently, the phased construction of dams in the upper reaches of the Mekong River has led to diminished downstream discharge at the Kratie station, causing episodic alterations in both runoff and water levels within the Tonle Sap Lake (Kallio and Kummu, 2021; Arias et al., 2014). In brief, variations in river-lake interactions could be a significant contributing factor to the observed changes in the water area and level of the Tonle Sap Lake over the past two decades.

Regarding the impact of dams and reservoirs within the Tonle Sap Lake basin, Cambodia has had limited infrastructure development due to past conflicts and political instability (Hoanh et al., 2012). As of 2020, there are a total of 16 dams in the Tonle Sap Lake basin, with only one of them, the Stung Battambang I Multipurpose dam, being operational in 2018. The operational dam has a relatively small reservoir capacity of 13 MW, while the remaining 15 dams are still in the planning phase (Open Development Mekong (ODM), 2021). Therefore, it is reasonable to assume that the impact of reservoirs on the lake's tributaries has been relatively minor over the past 20 years. In addition, Cambodia had a total of 10 reservoirs as of 2016, with the largest operational reservoir being the Stung Sen Upper Command reservoir located within the Tonle Sap Lake basin (Open Development Cambodia (ODC), 2016). While this reservoir accumulates a significant volume of water during the wet season and releases significant amounts of water during the dry season, its influence on the lake's annual variations is relatively limited. However, it may have some impacts on seasonal changes, such as water levels and flow patterns, within specific time frames. In summary, the construction of dams in the upper reaches of the Mekong River has significantly affected the downstream discharge at the Tonle Sap Lake, leading to episodic alterations in runoff and water levels. However, the impact of dams and reservoirs within the Tonle Sap Lake basin itself has been relatively minor over the past two decades, with limited operational dams and reservoirs in the area.

4.4. Expansion of agricultural land

In Cambodia, a significant portion of agricultural land, approximately 90 %, lies in the flood plains of the Mekong River and the Tonle Sap Lake (Mekong River Commission (MRC), 2011a). Over the past two decades, Cambodia has actively promoted the construction and maintenance of its irrigation system, with an estimated irrigation potential of 1.6 million hectares (Raju and Taron, 2018). Consequently, surface runoff in the Tonle Sap Lake basin and Mekong River basin is extensively utilized for irrigation purposes in Cambodia. Given that the discharge of the Mekong River flows into the Tonle Sap Lake via the Tonle Sap River, the impact of irrigation intensity on the Mekong River ultimately manifests in its effects on the Tonle Sap Lake. Here, despite the lack of specific data on the exact extent of irrigated agricultural land within the watershed, the total area of agricultural land can serve as an indicator of irrigation intensity. Until the end of 2017, there was a total of 2483 irrigation systems ranging from small to large scale across the country, with the capacity to irrigate 1,716,720 ha of arable land, accounting for 93 % of the nation's arable land (Ministry of water resources and meteorology (MOWRAM), 2018). In terms of agricultural land expansion, the average agricultural land area in the watershed increased from 5100×10^5 ha in the first period to 5412×10^5 ha in the second period and further grew to 5637×10^5 ha in the third phase (Fig. 12A). A noteworthy finding is the significant correlation ($R = 0.56$, $P < 0.05$) observed between annual agricultural land and the average annual area of the lake (Fig. 12B), highlighting the prominent role of agricultural land expansion in exacerbating the progressive shrinkage of the lake over time. This correlation may suggest that the expansion of agricultural activities contributes to the ongoing reduction in the extent of the lake. To further explore the relationships between the lake area, runoff in the Mekong River, and agricultural land, a multiple linear regression analysis was conducted using the average yearly runoff from the Kratie station on the Mekong River's mainstream and the average yearly agricultural land area. The regression equation is as follows:

$$Y = 5262.90 + 730.83X_1 - 26.67X_2 \quad (3)$$

where Y refers to the surface area of Tonle Sap Lake, X_1 refers to the runoff from the average yearly runoff at the Kratie hydrological station, and X_2 refers to the average yearly agricultural land area in Cambodia. Moreover, $Y, X_1 and X_2$ are standardized to eliminate the dimensional differences among data, respectively. The regression equation, yields a R^2 value of 0.84. Using the Multiple Linear Regression analysis method proposed by Larsen and Baker (2003) and standardizing the data, the relative contribution of each variable was calculated, resulting in a relative contribution of 96.48 % for X_1 and 3.52 % for X_2. While these values may not provide an absolute measure of influence, they suggest the relative weights of agricultural land expansion and Mekong River runoff on the annual fluctuations of the Tonle Sap Lake's water area. Notably, the effect of agricultural land on the lake surface area could be negligible in comparison to the impact from runoff. The regression analysis further demonstrates the relative contributions of agricultural land expansion and Mekong River runoff, with runoff exerting a more substantial influence on the lake area. However, a comparison between satellite images from the 2000s and 2020 reveals the conversion of forests into shrublands, and shrublands transforming into croplands, indicating that floodplains of the lake are gradually being occupied by agricultural land in the basin (Fig. 12C). This partially explains the correlation between the surface area of the lake and agricultural land.

Moreover, despite the shrinkage of the lake accompanying a decrease in water levels, the decline in water levels alone cannot fully explain the lake's changes. A detailed analysis of high-resolution lake imagery obtained through Google Earth Pro (Fig. 13) was conducted to determine the reasons behind the differential extent of shrinking along the eastern and western shorelines. In the western part of the lake, the presence of numerous tributaries and a meandering shoreline were observed (Fig. 13B), which could potentially lead to sediment accumulation at the edge of the lake (Lane, 2023). This sediment accumulation may result in a gradual increase in elevation at the lake edge year by year. Simultaneously, in the eastern part of the lake, we observed well-defined embankments and human-made reclamation efforts for the protection of the cultivated farmland, which may have contributed to decelerating the shrinking of the lake shoreline (Fig. 13C). From another perspective, the rate of shoreline shrinkage is closely linked to shoreline morphology. Furtherly, the expansion of agricultural land has a relatively modest impact on the shrinking of the lake; however, localized efforts in reclaiming farmland could impede the lake's recession in specific areas. These findings underscore the complex interactions between human activities, water resources management, and the ecological dynamics of the Tonle Sap Lake, emphasizing the need for integrated and sustainable approaches to mitigate the ongoing decline of the lake.

5. Conclusion

The Tonle Sap Lake, as the largest freshwater lake in Southeast Asia,

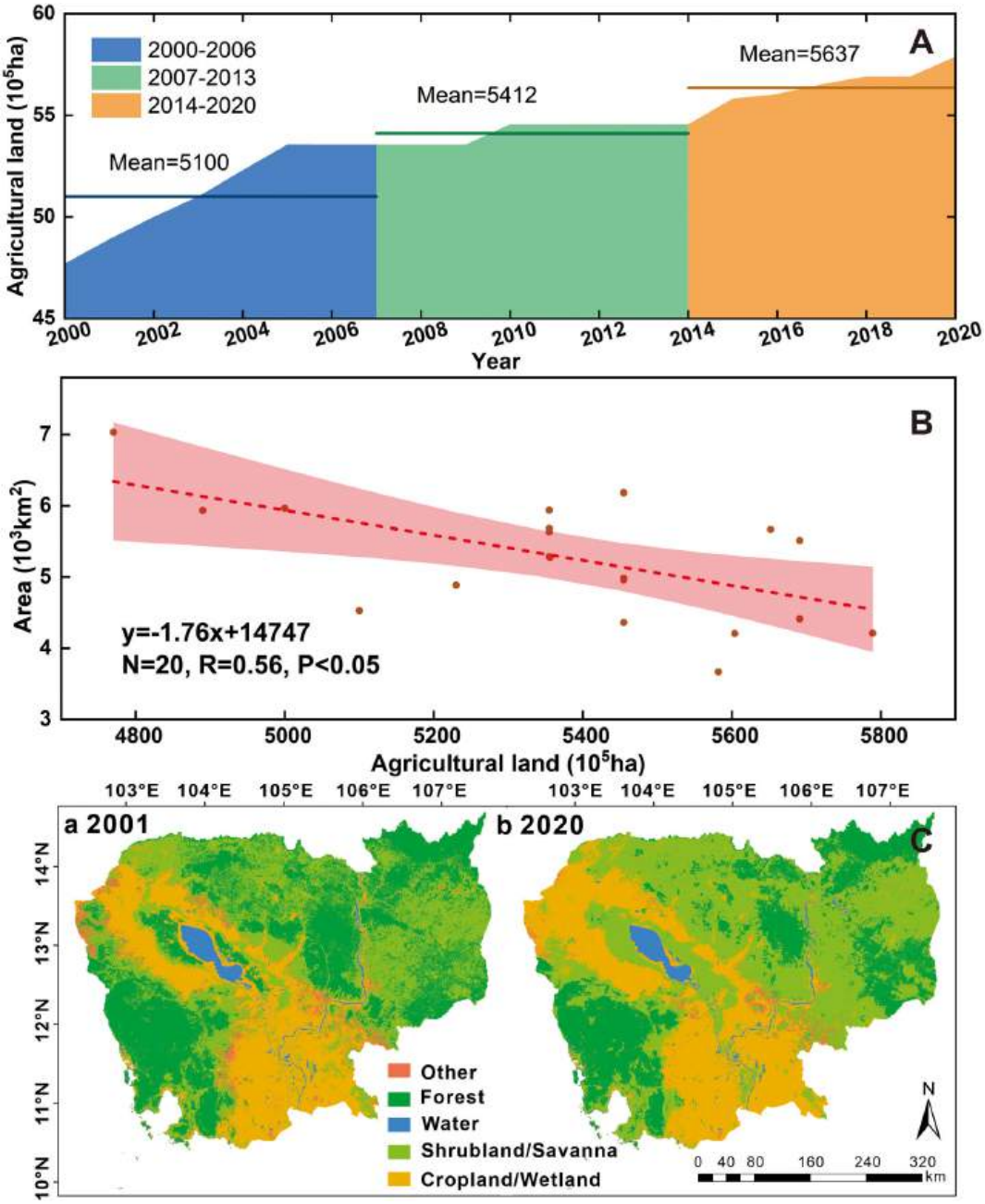

Fig. 12. A: Long-term annual mean agricultural land area of Cambodia from 2000 to 2020; B: Correlations between annual mean Agricultural land and the mean area of Cambodia (data from the World Bank) C: Comparison of land use of Cambodia in 2001 and 2020.

has attracted international attention due to its ongoing exacerbating decline, which aligns with the global trend of shrinking lakes. This decline in the lake is influenced by both climate change and human activities, which have disrupted the natural cycles of various elements. In this study, we explored the dynamics of the Tonle Sap Lake over the past two decades and clarified the possible causes of its variations. The main findings are summarized as follows:

1. From 2000 to 2020, the water level of the Tonle Sap Lake experienced an average annual decrease of 0.1 m, accompanied by an average yearly reduction of 66.85km^2 in surface area. Concurrently, during the dry season, the shoreline of the Tonle Sap Lake experienced a shrinkage a rate of 47 m/yr.
2. Despite the seasonal variations in the water level of the Tonle Sap Lake, there is distinct pattern of reduced flooding during the flood season and heightened aridity during the dry season. Similar changes are observed in the lake's surface area. These episodic declines in water level and surface area of the Tonle Sap Lake can be primarily attributed to intermittent dam construction upstream of the Mekong River.
3. The significant shrinkage observed in the northwestern and southeastern lake regions of the lake may be partially attributed to the sediment accumulation from numerous tributaries along the edge of the lake, resulting in shallower depth. In contrast, the eastern part of the lake has remained relatively stable, with consistent overlapping shorelines from multiple years, which can be partially attributed to the presence of well-defined artificial embankments.
4. The seasonal fluctuations of the lake are controlled by regional precipitation in the Mekong River basin, while the prolonged decrease in inflow to the Tonle Sap Lake is primarily linked to the

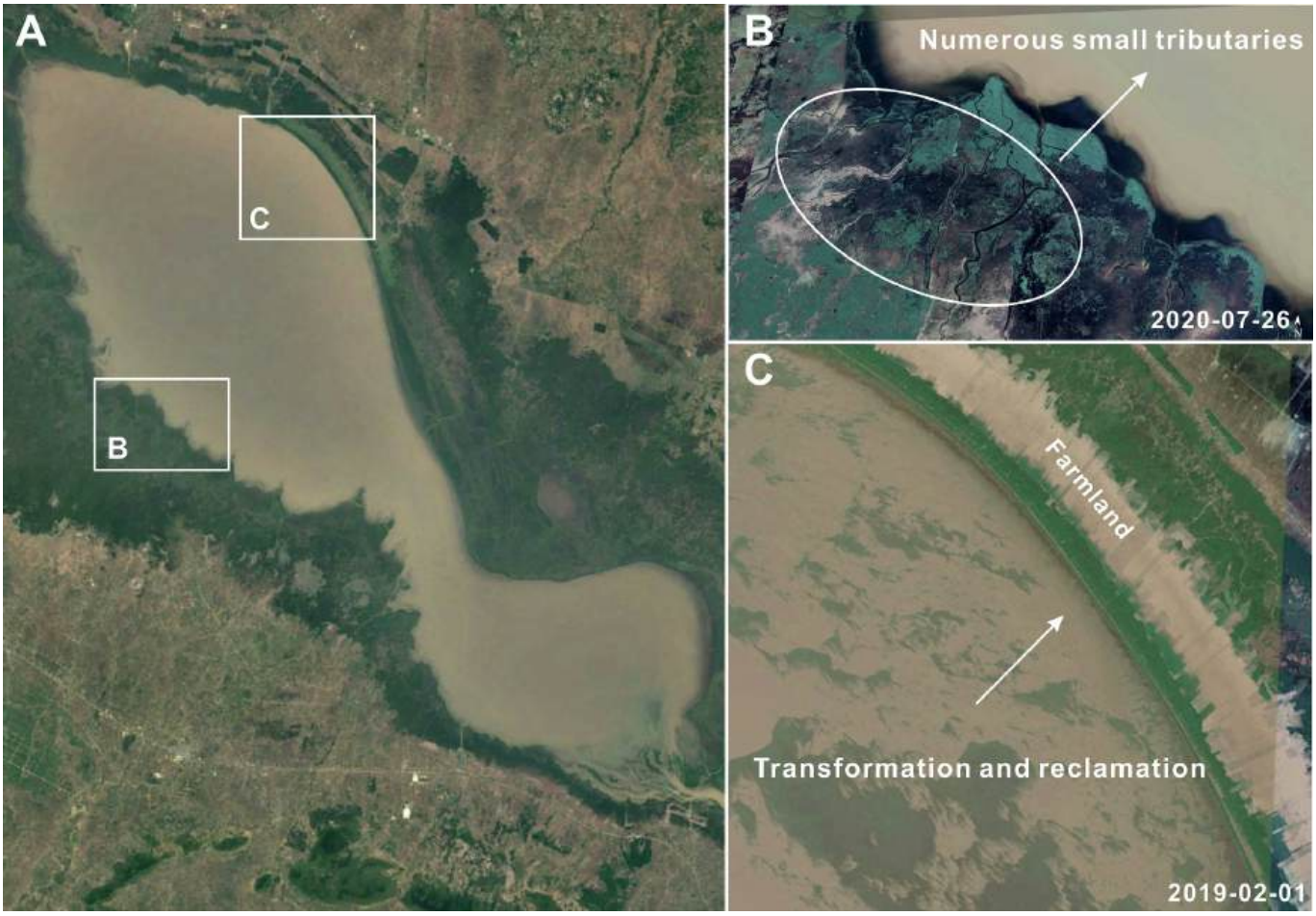

Fig. 13. Landscape features around the Tonle Sap Lake.

shrinkage caused by dams and interannual declines in rainfall within the Mekong River basin.

These findings highlight that the Tonle Sap Lake have experienced significant shrinkage as a result of intensified human activities, changes in Mekong River runoff, and dam construction in the upper Mekong River. The cumulative pressures on the Tonle Sap Lake place it at considerable risk, particularly in terms of its shrinking size. It is of utmost importance to prioritize the protection and conservation of the lake's shoreline, considering its ecological importance and the valuable services it provides. Considering the intensified construction of hydropower stations in the upstream Mekong River, which has already severely impacted the Tonle Sap Lake ecosystem, there is an urgent need to establish a resilient and environmentally friendly cross-regional solution that strikes a balance between dam construction and the lake's ecological safety. Moreover, the current water governance practices in Cambodia demonstrate weaknesses and fragmentation. In the western part of the lake, the creation of protective zones, reducing of deforestation in the surrounding hills, and enhancement of ecological resilience can contribute to water retention and minimize sediment accumulation in the vicinity of the lake. In the eastern part of the lake, the rational relocation of agricultural land can help maintain the existing shoreline. In conclusion, the findings of this study emphasize the substantial decline of the Tonle Sap Lake due to increased human activity, changes in Mekong River runoff, and dam construction. To safeguard the Tonle Sap Lake and its ecosystem, urgent measures are needed, including a comprehensive cross-regional approach to dam construction, improved water governance practices, optimized irrigation water management, and targeted interventions in specific regions of the lake.

CRediT authorship contribution statement

Wenting Jiang: Writing – original draft, Methodology, Investigation, Data curation. **Zhijun Dai:** Writing – review & editing, Writing – original draft, Validation, Supervision, Project administration, Methodology, Investigation, Funding acquisition, Data curation, Conceptualization. **Xuefei Mei:** Visualization, Software. **Chuqi Long:** Formal analysis, Data curation. **Nguyen An Binh:** Resources, Investigation. **Cong Mai Van:** Software, Resources. **Jinping Cheng:** Writing – review & editing, Investigation, Formal analysis.

Declaration of competing interest

The authors declare that there are no conflicts of interest regarding the submitted paper of "Profiling dynamics of the Southeast Asia's largest lake, Tonle Sap Lake".

Data availability

Data will be made available on request.

Acknowledgments

This research was supported by the National Natural Science Key Foundation of China (NSFC) (41930537), Shanghai International Science and Technology Cooperation Fund Project (23230713800; 19230742700).

References

Adrian, R., O'Reilly, C.M., Zagarese, H., Baines, S.B., Hessen, D.O., Keller, W., Winder, M., 2009. Lakes as sentinels of climate change. Limnol. Oceanogr. 54 (6part2), 2283–2297.

Alcocer, J., Lugo, A., 2003. Effects of El Niño on the dynamics of Lake Alchichica, Central Mexico. Geofis. Int. 42 (3), 523–528.

Arias, M.E., 2013. Impacts of Hydrological Alterations in the Mekong Basin to the Tonle Sap Ecosystem.

Arias, M.E., Cochrane, T.A., Piman, T., Kummu, M., Caruso, B.S., Killeen, T.J., 2012. Quantifying changes in flooding and habitats in the Tonle Sap Lake (Cambodia) caused by water infrastructure development and climate change in the Mekong Basin. J. Environ. Manag. 112, 53–66.

Arias, M.E., Piman, T., Lauri, H., Cochrane, T.A., Kummu, M., 2014. Dams on Mekong tributaries as significant contributors of hydrological alterations to the Tonle Sap floodplain in Cambodia. Hydrol. Earth Syst. Sci. 18 (12), 5303–5315.

Bonsal, B.R., Zhang, X., Vincent, L.A., Hogg, W.D., 2001. Characteristics of daily and extreme temperatures over Canada. J. Clim. 14 (9), 1959–1976.

Brönmark, C., Hansson, L.A., 2017. The Biology of Lakes and Ponds. Oxford University Press.

Caballero, I., Navarro, G., 2021. Monitoring cyanoHABs and water quality in Laguna Lake (Philippines) with Sentinel-2 satellites during the 2020 Pacific typhoon season. Sci. Total Environ. 788, 147700.

Campbell, I.C., Poole, C., Giesen, W., Valbo-Jorgensen, J., 2006. Species diversity and ecology of Tonle Sap great Lake, Cambodia. Aquat. Sci. 68, 355–373.

Chen, A., Liu, J., Kummu, M., Varis, O., Tang, Q., Mao, G., Chen, D., 2021. Multidecadal variability of the Tonle Sap Lake flood pulse regime. Hydrol. Process. 35 (9), e14327.

Chua, S.D.X., Lu, X.X., Oeurng, C., Sok, T., Grundy-Warr, C., 2022. Drastic decline of flood pulse in the Cambodian floodplains (Mekong River and Tonle Sap system). Hydrol. Earth Syst. Sci. 26 (3), 609–625.

Cochrane, T.A., Arias, M.E., Piman, T., 2014. Historical impact of water infrastructure on water levels of the Mekong River and the Tonle Sap system. Hydrol. Earth Syst. Sci. 18 (11), 4529–4541.

Cooley, S.W., 2023. Global loss of lake water storage. Science 380 (6646), 693.

Dang, H., Pokhrel, Y., Shin, S., Stelly, J., Ahlquist, D., Du Bui, D., 2022. Hydrologic balance and inundation dynamics of Southeast Asia's largest inland lake altered by hydropower dams in the Mekong River basin. Sci. Total Environ. 831, 154833.

Delgado, J.M., Apel, H., Merz, B., 2010. Flood trends and variability in the Mekong River. Hydrol. Earth Syst. Sci. 14 (3), 407–418.

Dore, M.H., 2005. Climate change and changes in global precipitation patterns: what do we know? Environ. Int. 31 (8), 1167–1181.

Du, Y., Xue, H.P., Wu, S.J., Ling, F., Xiao, F., Wei, X.H., 2011. Lake area changes in the middle Yangtze region of China over the 20th century. J. Environ. Manag. 92 (4), 1248–1255.

Eyler, B., 2020. Science shows Chinese dams are devastating the Mekong. Foreign Policy 22.

Foga, S., Scaramuzza, P.L., Guo, S., Zhu, Z., Dilley Jr., R.D., Beckmann, T., Laue, B., 2017. Cloud detection algorithm comparison and validation for operational Landsat data products. Remote Sens. Environ. 194, 379–390.

Frappart, F., Biancamaria, S., Normandin, C., Blarel, F., Bourrel, L., Aumont, M., Darrozes, J., 2018. Influence of recent climatic events on the surface water storage of the Tonle Sap Lake. Sci. Total Environ. 636, 1520–1533.

Gao, J., Dai, Z., Mei, X., Ge, Z., Wei, W., Xie, H., Li, S., 2015. Interference of natural and anthropogenic forcings on variations in continental freshwater discharge from the Red River (Vietnam) to sea. Quat. Int. 380, 133–142.

Grant, L., Vanderkelen, I., Gudmundsson, L., Tan, Z., Perroud, M., Stepanenko, V.M., Thiery, W., 2021. Attribution of global lake systems change to anthropogenic forcing. Nat. Geosci. 14 (11), 849–854.

Gronewold, A.D., Stow, C.A., 2014. Water loss from the Great Lakes. Science 343 (6175), 1084–1085.

Gu, Z., Zhang, Y., Fan, H., 2021. Mapping inter-and intra-annual dynamics in water surface area of the Tonle Sap Lake with Landsat time-series and water level data. J. Hydrol. 601, 126644.

Hoanh, C.T., Facon, T., Thuon, T., Bastakoti, R.C., Molle, F., Phengphaengsy, F., 2012. Irrigation in the lower Mekong Basin countries: The beginning of a new era?. In: Contested Waterscapes in the Mekong Region. Routledge, pp. 143–171.

Huete, A., Didan, K., Miura, T., Rodriguez, E.P., Gao, X., Ferreira, L.G., 2002. Overview of the radiometric and biophysical performance of the MODIS vegetation indices. Remote Sens. Environ. 83 (1–2), 195–213.

Humphries, M.S., Green, A.N., Finch, J.M., 2016. Evidence of El Niño driven desiccation cycles in a shallow estuarine lake: the evolution and fate of Africa's largest estuarine system, Lake St Lucia. Glob. Planet. Chang. 147, 97–105.

Intergovernmental Panel on Climate Change (IPCC), 2007. In: Solomon, S., et al. (Eds.), Climate Change 2007: The Physical Science Basis-Contribution of Working Group I to the Fourth Assessment Report of the Intergovernmental Panel on Climate Change. Cambridge Univ. Press, Cambridge, U. K, pp. 663–745.

Ji, L., Gong, P., Wang, J., Shi, J., Zhu, Z., 2018a. Construction of the 500-m resolution daily global surface water change database (2001–2016). Water Resour. Res. 54 (12), 10–270.

Ji, X., Li, Y., Luo, X., He, D., 2018b. Changes in the lake area of Tonle Sap: possible linkage to runoff alterations in the Lancang River? Remote Sens. 10 (6), 866.

Junk, W.J., Bayley, P.B., Sparks, R.E., 1989. The flood pulse concept in river-floodplain systems. Can. J. Fish. Aquat. Sci. 106 (1), 110–127.

Kallio, M., Kummu, M., 2021. Comment on 'changes of inundation area and water turbidity of Tonle Sap Lake: responses to climate changes or upstream dam construction?'. Environ. Res. Lett. 16 (5), 058001.

Karlsson, J., Jonsson, A., Jansson, M., 2005. Productivity of high-latitude lakes: climate effect inferred from altitude gradient. Glob. Chang. Biol. 11 (5), 710–715.

Knoll, L.B., Sharma, S., Denfeld, B.A., Flaim, G., Hori, Y., Magnuson, J.J., Weyhenmeyer, G.A., 2019. Consequences of lake and river ice loss on cultural ecosystem services. Limnol. Oceanogr. Lett. 4 (5), 119–131.

Kuenzer, C., 2014. Remote sensing the Mekong. Int. J. Remote Sens. 35 (8), 2747–2751.

Kummu, M., Penny, D., Sarkkula, J., Koponen, J., 2008. Sediment: curse or blessing for Tonle Sap Lake? AMBIO: J. Human Environ. 37 (3), 158–163.

Kummu, M., Tes, S., Yin, S., Adamson, P., Józsa, J., Koponen, J., Sarkkula, J., 2014. Water balance analysis for the Tonle Sap Lake–floodplain system. Hydrol. Process. 28 (4), 1722–1733.

Lane, R.K., 2023. Lake. Encyclopedia Britannica. https://www.britannica.com/science/lake.

Larsen, R.K., Baker, J.E., 2003. Source apportionment of polycyclic aromatic hydrocarbons in the urban atmosphere: a comparison of three methods. Environ. Sci. Technol. 37 (9), 1873–1881.

Lauri, H., de Moel, H., Ward, P.J., Räsänen, T.A., Keskinen, M., Kummu, M., 2012. Future changes in Mekong River hydrology: impact of climate change and reservoir operation on discharge. Hydrol. Earth Syst. Sci. 16 (12), 4603–4619.

Lee, D.E., Jung, S.H., Yeon, M.H., Lee, G.H., 2021. Analysis of future flood inundation change in the Tonle Sap basin under a climate change scenario. Korean J. Agric. Sci. 48 (3), 433–446.

Li, Y., Zhang, Q., Werner, A.D., Yao, J., Ye, X., 2017. The influence of river-to-Lake backflow on the hydrodynamics of a large floodplain lake system (Poyang lake, China). Hydrol. Process. 31 (1), 117–132.

Long, C., Dai, Z., Wang, R., Lou, Y., Zhou, X., Li, S., Nie, Y., 2022. Dynamic changes in mangroves of the largest delta in northern Beibu gulf, China: reasons and causes. For. Ecol. Manag. 504, 119855.

Lou, Y., Dai, Z., Long, C., Dong, H., Wei, W., Ge, Z., 2022. Image-based machine learning for monitoring the dynamics of the largest salt marsh in the Yangtze River Delta. J. Hydrol. 608, 127681.

Lu, X.X., Li, S., Kummu, M., Padawangi, R., Wang, J.J., 2014. Observed changes in the water flow at Chiang Saen in the lower Mekong: impacts of Chinese dams? Quat. Int. 336, 145–157.

Mei, X., Dai, Z., Du, J., Chen, J., 2015. Linkage between Three Gorges Dam impacts and the dramatic recessions in China's largest freshwater lake. Poyang Lake. Sci. Rep. 5 (1), 18197.

Mekong River Commission (MRC), 2005. MRC Annual Report 2005. MRC Secretariat, Vientiane.

Mekong River Commission (MRC), 2011a. Agriculture and Irrigation Programme (AIP) 2011–2015.

Mekong River Commission (MRC), 2011b. MRC Annual Report 2010. MRC Secretariat, Vientiane.

Mendonça, R., Müller, R.A., Clow, D., Verpoorter, C., Raymond, P., Tranvik, L.J., Sobek, S., 2017. Organic carbon burial in global lakes and reservoirs. Nat. Commun. 8 (1), 1694.

Micklin, P., 2010. The past, present, and future Aral Sea. Lakes Reserv. Res. Manag. 15 (3), 193–213.

Ministry of water resources and meteorology (MOWRAM), 2018. http://www.cambodiameteo.com/.

Morovati, K., Tian, F., Kummu, M., Shi, L., Tudaji, M., Nakhaei, P., Olivares, M.A., 2023. Contributions from climate variation and human activities to flow regime change of Tonle Sap Lake from 2001 to 2020. J. Hydrol. 616, 128800.

Ng, W.X., Park, E., 2021. Shrinking Tonlé sap and the recent intensification of sand mining in the Cambodian Mekong River. Sci. Total Environ. 777, 146180.

Nuorteva, P., Keskinen, M., Varis, O., 2010. Water, livelihoods and climate change adaptation in the Tonle Sap Lake area, Cambodia: learning from the past to understand the future. J. Water Clim. Chang. 1 (1), 87–101.

Nyland, E., Gunn, E., Shiklomanov, I., Engstrom, N., Streletskiy, A., 2018. Land cover change in the lower Yenisei River using dense stacking of landsat imagery in Google earth engine. Remote Sens. 10 (8), 1226.

Oeurng, C., Cochrane, T.A., Chung, S., Kondolf, M.G., Piman, T., Arias, M.E., 2019. Assessing climate change impacts on river flows in the Tonle Sap Lake Basin, Cambodia. Water 11 (3), 618.

Okin, G.S., Gu, J., 2015. The impact of atmospheric conditions and instrument noise on atmospheric correction and spectral mixture analysis of multispectral imagery. Remote Sens. Environ. 164, 130–141.

Open Development Cambodia (ODC), 2016. https://opendevelopmentcambodia.net/profiles/reservoir/.

Open Development Mekong (ODM), 2021. https://data.opendevelopmentmekong.net/en/dataset/mekong-regional-hydropower-dams-2020.

O'Reilly, C.M., Sharma, S., Gray, D.K., Hampton, S.E., Read, J.S., Rowley, R.J., Zhang, G., 2015. Rapid and highly variable warming of lake surface waters around the globe. Geophys. Res. Lett. 42 (24), 10–773.

Penny, D., Cook, G., Im, S.S., 2005. Long-term rates of sediment accumulation in the Tonle Sap, Cambodia: a threat to ecosystem health? J. Paleolimnol. 33, 95–103.

Peter, H.G., 1993. Water and conflict: fresh water resources and international security. Int. Secur. 18 (1), 79.

Raju, K.V., Taron, A., 2018. Enabling Sustainable and Inclusive Irrigation Development in Cambodia.

Räsänen, T.A., Kummu, M., 2013. Spatiotemporal influences of ENSO on precipitation and flood pulse in the Mekong River basin. J. Hydrol. 476, 154–168.

Rouse, J.W., Haas, R.H., Schell, J.A., Deering, D.W., 1974. Monitoring vegetation systems in the Great Plains with ERTS. NASA Spec. Publ 351 (1), 309.

Siev, S., Paringit, E.C., Yoshimura, C., Hul, S., 2016. Seasonal changes in the inundation area and water volume of the Tonle Sap River and its floodplain. Hydrology 3 (4), 33.
Sok, T., Oeurng, C., Kaing, V., Sauvage, S., Kondolf, G.M., Sánchez-Pérez, J.M., 2021. Assessment of suspended sediment load variability in the Tonle Sap and lower Mekong Rivers, Cambodia. Catena (Amst) 202, 105291.
Stager, J.C., Ruzmaikin, A., Conway, D., Verburg, P., Mason, P.J., 2007. Sunspots, El Nino, and the levels of Lake Victoria, East Africa. J. Geophys. Res. Atmos. 112 (D15).
Tang, R., Dai, Z., Mei, X., Zhou, X., Long, C., Van, C.M., 2023. Secular trend in water discharge transport in the lower Mekong River-delta: effects of multiple anthropogenic stressors, rainfall, and tropical cyclones. Estuar. Coast. Shelf Sci. 281, 108217.
Tao, S., Fang, J., Zhao, X., Zhao, S., Shen, H., Hu, H., Guo, Q., 2015. Rapid loss of lakes on the Mongolian Plateau. Proc. Natl. Acad. Sci. U. S. A. 112 (7), 2281–2286.
Tian, B., Gao, P., Mu, X., Zhao, G., 2023. Water area variation and river–lake interactions in the Poyang Lake from 1977–2021. Remote Sens. 15 (3), 600.
Tsukawaki, S., 1997, August. Lithological features of cored sediments from the northern part of Lake Tonle Sap, Cambodia. In: Proceedings of the International Conference on Stratigraphy and Tectonic Evolution of Southeast Asia and the South Pacific. Dept Min Res., Bangkok, Thailand, pp. 232–239.
Wang, W., Lu, H., 2015. Evaluation and hydrological applications of TRMM rainfall products over the Mekong River basin with a distributied model. In: In 2015 IEEE International Geoscience and Remote Sensing Symposium (IGARSS). IEEE, pp. 2511–2514.
Wang, Y., Feng, L., Liu, J., Hou, X., Chen, D., 2020. Changes of inundation area and water turbidity of Tonle Sap Lake: responses to climate changes or upstream dam construction? Environ. Res. Lett. 15 (9), 0940a1.
Wei, Fengying, 1999. Modern Climate Statistical Diagnosis and Prediction Technology. China Meteorological Press, Beijing.
Woolway, R.I., Kraemer, B.M., Lenters, J.D., Merchant, C.J., O'Reilly, C.M., Sharma, S., 2020. Global lake responses to climate change. Nat. Rev. Earth Environ. 1 (8), 388–403.
Wu, S., Ishidaira, H., Sun, W., 2009. Potential impact of Sambor dam project on interaction between Mekong River and Tonle Sap Lake. Environ. Res. 2009.
Wu, F., Wang, X., Cai, Y., Li, C., 2016. Spatiotemporal analysis of precipitation trends under climate change in the upper reach of Mekong River basin. Quat. Int. 392, 137–146.
Wurtsbaugh, W.A., Miller, C., Null, S.E., DeRose, R.J., Wilcock, P., Hahnenberger, M., Moore, J., 2017. Decline of the world's saline lakes. Nat. Geosci. 10 (11), 816–821.
Xiao, M., Zhang, Q., Singh, V.P., 2015. Influences of ENSO, NAO, IOD and PDO on seasonal precipitation regimes in the Yangtze River basin, China. Int. J. Climatol. 35 (12), 3556–3567.
Xu, H., 2006. Modification of normalised difference water index (NDWI) to enhance open water features in remotely sensed imagery. Int. J. Remote Sens. 27 (14), 3025–3033.
Yao, F., Livneh, B., Rajagopalan, B., Wang, J., Crétaux, J.F., Wada, Y., Berge-Nguyen, M., 2023. Satellites reveal widespread decline in global lake water storage. Science 380 (6646), 743–749.
Yechieli, Y., Gavrieli, I., Berkowitz, B., Ronen, D., 1998. Will the Dead Sea die? Geology 26 (8), 755–758.
Yin, H., Liu, G., Pi, J., Chen, G., Li, C., 2007. On the river–lake relationship of the middle Yangtze reaches. Geomorphol. (Amst) 85 (3–4), 197–207.
Zhang, Q., Li, L., Wang, Y.G., Werner, A.D., Xin, P., Jiang, T., Barry, D.A., 2012. Has the three-gorges dam made the Poyang Lake wetlands wetter and drier? Geophys. Res. Lett. 39 (20).
Zhang, J., Fan, H., He, D., Chen, J., 2019. Integrating precipitation zoning with random forest regression for the spatial downscaling of satellite-based precipitation: A case study of the Lancang-Mekong River basin. Int. J. Climatol. 39 (10), 3947–3961.
Zhao, G., Li, Y., Zhou, L., Gao, H., 2022. Evaporative water loss of 1.42 million global lakes. Nat. Commun. 13 (1), 3686.
Zhou, Y., Dong, J., Xiao, X., Liu, R., Zou, Z., Zhao, G., Ge, Q., 2019. Continuous monitoring of lake dynamics on the Mongolian plateau using all available Landsat imagery and Google earth engine. Sci. Total Environ. 689, 366–380.